Best
Available
Copy

AD-784 911

SURFACE WAVE STUDIES ON CRUSTAL AND MANTLE STRUCTURE OF CHINA

James P. Tung, et al

University of Southern California

Prepared for:

Air Force Office of Scientific Research
Advanced Research Projects Agency

1974

REPORT DOCUMENTATION PAGE		READ INSTRUCTIONS BEFORE COMPLETING FORM
1. REPORT NUMBER AFOSR - TR - 74 - 1942	2. GOVT ACCESSION NO.	3. RECIPIENT'S CATALOG NUMBER AD-784911
4. TITLE (and Subtitle) Surface Wave Studies on Crustal and Mantle Structure of China		5. TYPE OF REPORT & PERIOD COVERED Scientific.....Interim
		6. PERFORMING ORG. REPORT NUMBER Tech Report 74-2
7. AUTHOR(s) James P. Tung and Ta-Liang Teng		8. CONTRACT OR GRANT NUMBER(s) AFOSR-74-2606
9. PERFORMING ORGANIZATION NAME AND ADDRESS University of Southern California Geophysical Laboratory Los Angeles, CA		10. PROGRAM ELEMENT, PROJECT, TASK AREA & WORK UNIT NUMBERS 62701E AO 1827
11. CONTROLLING OFFICE NAME AND ADDRESS Advanced Research Projects Agency/NMR 1400 Wilson Blvd Arlington, VA 22209		12. REPORT DATE July 1974
		13. NUMBER OF PAGES 56
14. MONITORING AGENCY NAME & ADDRESS(if different from Controlling Office) Air Force Office of Scientific Research/NP 1400 Wilson Blvd Arlington, VA 22209		15. SECURITY CLASS. (of this report) UNCLASSIFIED
		15a. DECLASSIFICATION/DOWNGRADING SCHEDULE

16. DISTRIBUTION STATEMENT (of this Report)

Approved for public release; distribution unlimited.

17. DISTRIBUTION STATEMENT (of the abstract entered in Block 20, if different from Report)

18. SUPPLEMENTARY NOTES

19. KEY WORDS (Continue on reverse side if necessary and identify by block number)
Multiple-filter
WWSSN
High-grain
Tibetan platform
South China platform

20. ABSTRACT (Continue on reverse side if necessary and identify by block number)
Multiple-filter technique has been applied to long-period WWSSN and high-grain records of earthquakes in the southeastern Asia to extract group velocity dispersion. Seismograms of surface wavepaths crossing Tibetan platform and South China platform have been used to obtain local crustal and upper mantle structures. It is found that when the multiple-filter technique is applied, the parameter in the Gaussian filter should vary linearly with frequency in order to avoid severe interference between the fundamental mode and later arrivals. Very low group velocities are obtained from wavepath across Tibetan platform in the periods

DD FORM
1 JAN 73 1473   EDITION OF 1 NOV 55 IS OBSOLETE

range of 10 sec. to 120 sec. which corresponds to an unusually thick crust of about 70 km and lower shear velocities in the upper mantle. Group velocities in the South China platform are close to an average continental structure with a crustal thickness of about 37 km. Group velocities of wavepath crossing the entire southern China are found to be equivalent to the values calculated by path-length weighted mean method from the low values of the Tibetan Platform and the high values of the South China Platform. This has experimentally confirmed that the regionalization is indeed a valid scheme at least within our experimental errors.

UNIVERSITY OF SOUTHERN CALIFORNIA
GEOPHYSICAL LABORATORY
TECHNIQUE REPORT NUMBER 74-2

Short Title of Work: Surface Wave Studies on Crustal
                                        and Mantle Structure of China

                                        By: James P. Tung and Ta-liang Teng

Contractor: University of Southern California

Principal Investigator: Professor Ta-liang Teng
        and   (213) 746-6124
Program Manager

Contract Number: AFOSR-74-2606

Effective Date of Contract: October 1, 1973

Contract Expiration Date: September 30, 1974
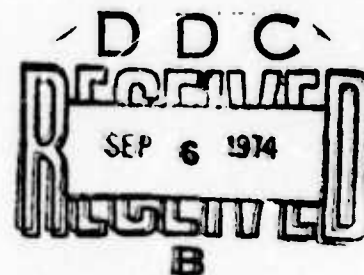
Amount of Contract: $19,002.00

Sponsored by: ARPA Order No. 1827,
                                        Program Code: 4F10

TABLE OF CONTENTS

iv

I ABSTRACT

Multiple-filter technique has been applied to long-period WWSSN and high-grain records of earthquakes in the southeastern Asia to extract group velocity dispersion. Seismograms of surface wavepaths crossing Tibetan platform and South China platform have been used to obtain local crustal and upper mantle structures.

It is found that when the multiple-filter technique is applied, the parameter α in theGaussian filter should vary linearly with frequency in order to avoid severe interference between the fundamental mode and later arrivals.

Very low group velocities are obtained from wavepath across Tibetan platform in the periods range of 10 sec. to 120 sec. which corresponds to an unusually thick crust of about 70 km and lower shear velocities in the upper mantle. Group velocities in the South China platform are close to an avearage continental structure with a crustal thickness of about 37 km.

Group velocities of wavepath crossing the entire southern China are found to be equivalent to the values calculated by path-length weighted mean method from the low values of the Tibetan Platform and the high values of the South China Platform. This has experimentally confirmed that the regionalization is indeed a valid scheme at least within our experimental errors.

1.

II. ACKNOWLEDGEMENT

III INTRODUCTION

Owing to its inaccessibility to the western scientist during the recent decades, little has been known about the crustal and upper mantle structure in the area of China. Yet, China occupies a huge portion of the Eurasia continent, any conclusions about the earth's crustal and upper mantle will not be complete without the knowledge of this area.

Over the past 12 years, the availability of long-period data gathered by the World-wide Standardized Seismorgraphic Network (WWSSN) and data from the newly established high-gain stations distributed around the periphery of Asia, plus the recent development of surface-wave enhancement techniques, make it very attractive to study the crustal and upper mantle structures of Mainland China by using surface waves.

In this report, results of our studies on the crustal and upper mantle structure in the southern China will be presented . The group velocity dispersion data are obtained by multiple-filtering technique developed recently by Dziewonski et al (1969).

Several tectonic terrains delineated principally by their current state of mobility and their relation to the principal tectonic cycle have been recognized in Eurasia (U.S. Geol. Survey Atlas, 1966). Those in the Mainland China are the (1) Central Asian fold system, (2) North China Korean platform, (3) Central China fold system, (4) Tibetan platform, (5) Indo-China fold system, (6) South China platform, and (7) the Cathaysian fold system (Fig. 1).

The platforms are stable segments of the continental crust characterized chiefly by epeirogenic distrophism, and are mostly in pre-phanerozoic time. They usually are composed of a pre-Paleozoic basement of crystalline and metamorphic rocks covered by flat-lying or gently dipping Paleozoic or younger sedimentaryrocks, accompanied by Mesozoic and Cenozoic faulting and volcanism.
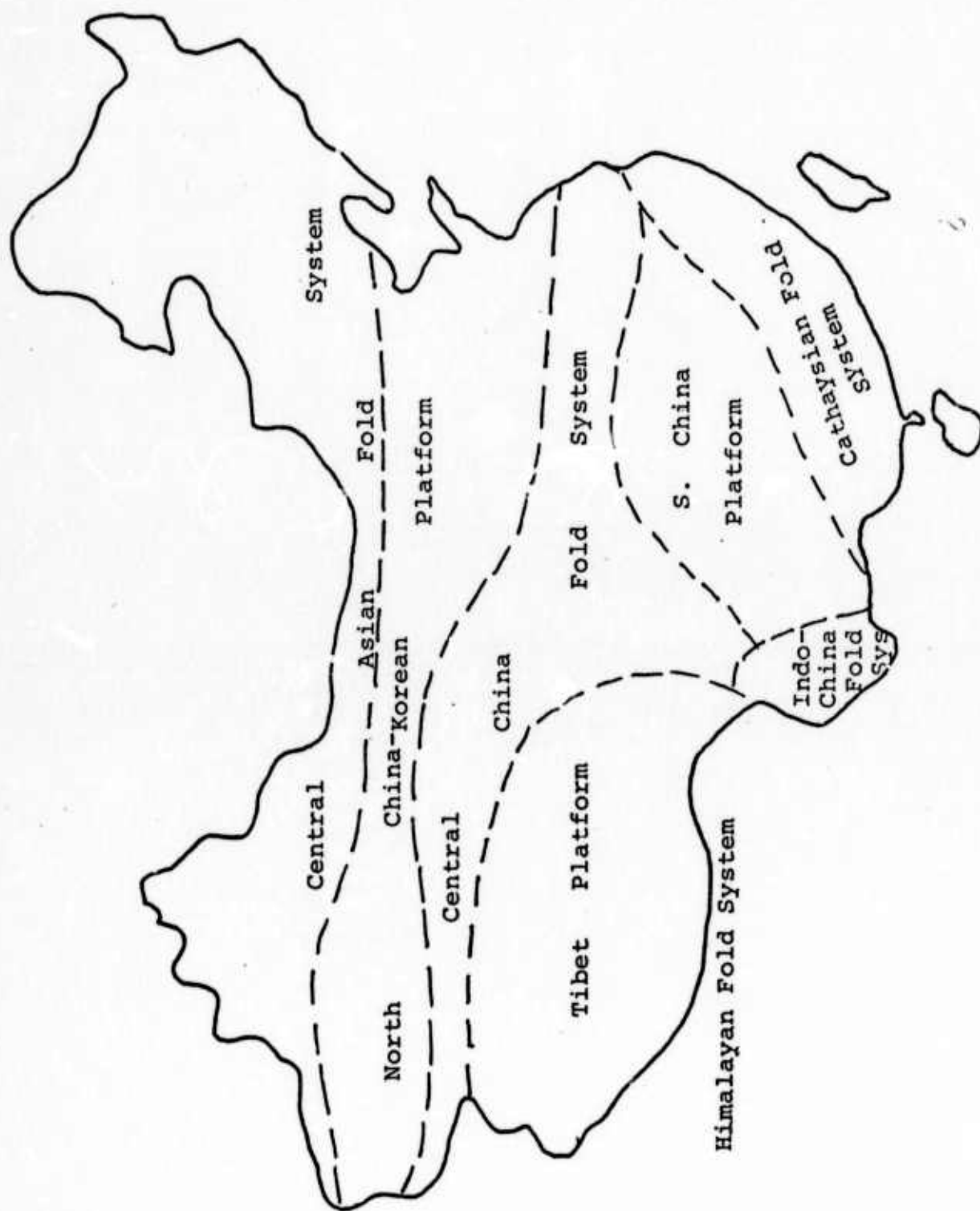
Figure 1 : Principal geological provinces in the Mainland China.

4.

Fold systems are mobile segments of the continental crust which have undergone an entire tectonic cycle within Phanerozoic time, and are characterized by intense orogenic diastrophism. They consist of uplifted basement with strongly metamorphosed gneiss and schist with some Paleozoic limestone. Weakly metamorphosed phyllite, slate, and sandstone are widespread. In addition, there are some scattered granitic and ultramafic rocks.

Southern China includes (1) Tibetan platform, (2) South China platform and (3) the Cathaysian fold system.

Figure 2 shows earthquakes epicenters and the wavepaths to the WWSSN station used in this study. Table 1 summarized earthquakes and their locations.
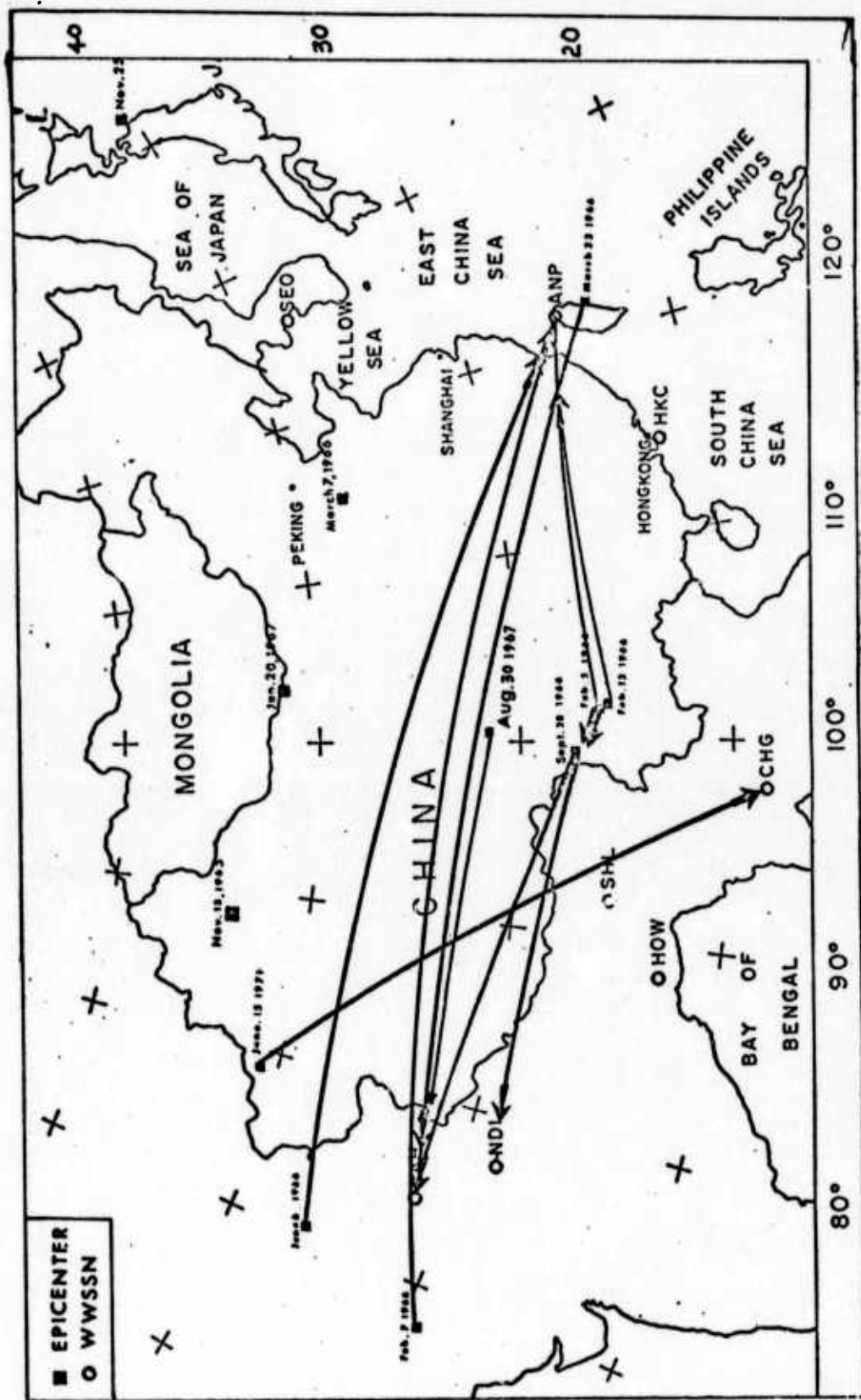
Earthquake	Latitude	Longitude	Magnitude	Recording Station
Sept. 28, 1966	27.5° N	100.0° E	6.1	LAH, NDI
Feb. 5, 1966	26.2° N	103.1° E	6.0	ANP, LAH, NDI
Feb. 7, 1966	29.9° N	69.7° E	6.0	ANP
Feb. 13, 1966	26.1° N	103.2° E	6.2	ANP
March 23, 1966	23.9° N	122.9° E	6.6	LAH, SHI
June 6, 1966	36.4° N	71.1° E	6.2	ANP
Aug. 30, 1967	31.7° N	100.3° E	6.1	LAH
June 15, 1971	41.5° N	79.3° E	5.6	CHG

Table I Earthquakes and recording stations used in our studies of Southern China.

7.

IV METHOD OF STUDY

Seismogram enlarged from film chips are first subjected to the following procedures:

1. Digitization

2. Multiple-filtering

Digitization

The seismogram is digitized using a Calma digitizer (Fig. 3). Before digitizing, a zero-line is visually drawn on the seismogram in such a way that (1) it is parallel to the general trend of all the traces on the seismogram; (2) its distance to the two adjacent traces are equal to the distance between other traces. The interval of digitization is predetermined so that only the sigment of the seismogram corresponding to group velocities from 4.5 km/sec to 2.0 km/sec is digitized. The length of surface wave train so determined ranges from 8 minutes to 20 minutes depending on the epicnetral distance. Digitized seismograms are plotted to make sure that there is no tilting, distortion, or zero-line shifting during the digitization process nad then the data are stored on cards and on magnetic tape.

Multiple Filtering

A digitized seismogram is first transformed using a fast fourier transform algorithm (Cooley &Tukey, 1965). After instrument correction, the complex spectrum is subjected to filtering in the frequency domain by a symmetrical, zero-phase-shift, Gaussian filter of the form:

$$F(\omega) = \exp\left[-\alpha\left(\frac{\omega - \omega_0}{\omega_0}\right)^2\right]$$

in which, ω_0 is center frequency, ω is variable frequency, α is a parameter which controls the roll-off and the width of the filter band. The
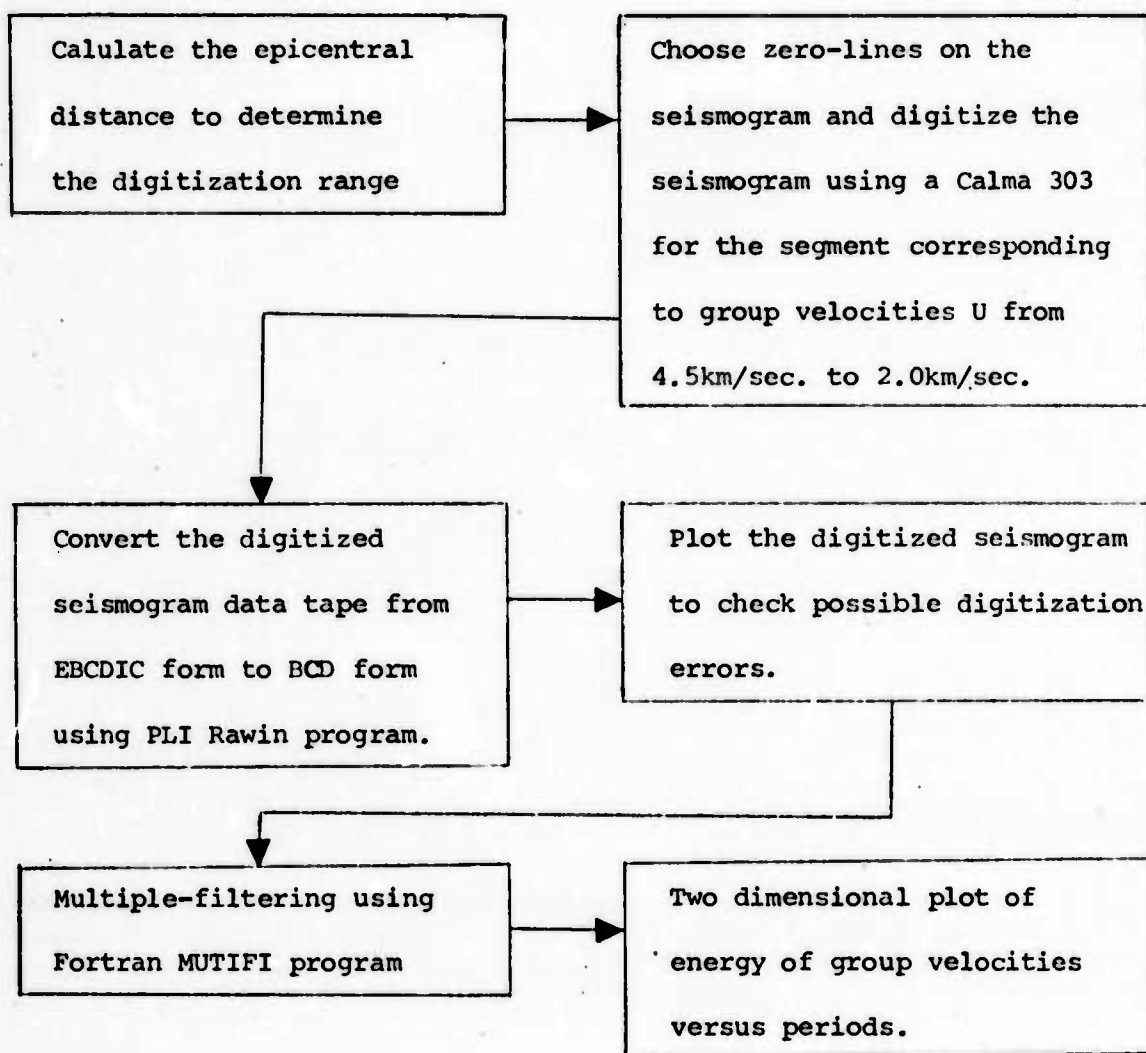
8.

Figure 3

Flow chart showing the procedures of obtaining
observed group velocities.

The frequency spectrum is then inverse transformed back to the time domain to give instantaneous amplitudes. The arrival time of the maximum amplitude corresponds to the group arrival time for the center frequency ω_o. This same process is repeated for different center frequencies to give the corresponding group arrivals. The result of the analysis of the entire frequency range gives the observed group velocity dispersion (Fig. 3 shows the Flow Chart of the data analysis procedures.)

In our study, the parameter α is set to be a function of frequency ω and epicentral distance for the following reasons: It was shown by Dziewonski and Hales (1972), and Hermann (1973) that the damping of the amplitude in the time domain by the Gaussian filter is

$$\exp \left[\omega_o^2 (t-t_o)^2/4\alpha\right]$$

Large value of α implies smaller damping for the time-domain signals. According to <u>uncertain principle</u> (Papouli, 1962), the duration of a signal in the time-domain is roughly a reciprocal of the width in the frequency domain for a function of Gaussian variation. If the bandwith is narrow in the frequency domain the duration in the time domain will be broad. For a single mode monotonic dispersion without later surface wave arrivals, the width of the time pulse does not affact the position of amplitude maximum, or the group arrivals. On most realistic seismograms, however, both higher-mode surface waves and later arrivals are present. Those arrivals will give several amplitude maxima in the time domain. The width of each of these peaks will depend on frequency, damping effect of the earth and the roll-off factor α in the Gaussian filter. If the duration of each of these maxima is long, and their relative arrival times are short, interference could occur(Dziewonski and Landisman, 1969; Herrmann, 1973). In fact, Herrmann (1973) shows that in order for two signals not to interfere severely with each other, the arrival

time difference should be $T_d = 2 T_o \sqrt{\frac{\alpha}{\pi}}$ or greater. This relationship can be understood since the arrival times of each mode and later arrivals are determined by the wave-path structure. The damping parameter α is at our disposal. It can be put in the following form:

$$\alpha = (t_d^2\ \pi)/(4T_o^2)$$

which is to say that if the two modes are arriving at t_d time apart, α should be equal to or less than the value given by this relation to avoid severe interference. It is seen from this relationship that α should be proportional to the square of frequency, instead of being a constant as set by Dziewonski et. al. (1969). However, if we substitute (2) into relation (1), the damping effect in the time-domain becomes constant over frequency, which is contrary to what have been found (Anderson et. al., 1965; Kanamori, 1970; Solomon, 1972). The attenuation of surface wave can be expressed by $\exp\lfloor -\gamma\Delta\rfloor$ where $\gamma = \pi/(TUQ)$ with Q being the attenuation quality factor, U the group velocity, T the period, and Δ the epicentral distance. If we assume U and Q are slowly varying (Anderson et. al., 1965; Kanamori, 1970; Solomon, 1972), the damping factor γ is close to a linear function of the frequency. Since the relative arrival times depend on the epicentral distance, α is set to be proportional to both frequency and epicentral distance:

$$\alpha = c\ \Delta\ \omega_b$$

11.

V. THEORETICAL MODEL CALCULATIONS

A computer program applying an algorithm of Takeuchi and Dorman (1964) was used to calculate the theoretical dispersions from a layered earth model. In this method, differential equations of motion are integrated from a depth about twice as the wave length to free surface. With the customary boundary conditions, these fundamental equations are transformed into a set of energy integrals from which the group velocity can be calculated.

For the Love wave problem, the energy integrals that are equivalent to the fundamental equations and the boundary conditions are:

$$(\sigma a)^2 I_1 + I_2 - N^2 I_3 = 0$$

in which σ is angular frequency, a earth's radius $N^2 = n(n + 1)$

$$I_1 = \int_c^1 \rho r^2 y_1^2 \, dr$$

$$I_2 = \int_c^1 \mu \, (y_1^2 + 2ry_1\dot{y}_1 - r^2\dot{y}_1^2) \, dr$$

$$I_3 = \int_0^1 \mu \, y_1^2 \, dr$$

and the group velocity is calculated by the formula:

$$U = I_3/cI_1$$

For Rayleigh wave problem without self-gravitation, the corresponding integrals are:

$$(\sigma a)^2 (I_1 + N^2 I_2) - (I_3 + I_6) + (2I_4 - I_7) N^2 - (I_5 + 2I_8)N^4 = 0 \quad \text{in which}$$

$$I_1 = \int_c^1 \rho r^2 y_1^2 dr$$

$$I_2 = \int_0^1 \rho r^2 y_3^2 dr$$

$$I_3 = \int_0^1 \lambda (r\dot{y}_1 + 2y_1)^2 dr$$

$$I_4 = \int_c^1 \lambda (r\dot{y}_1 + 2y_1) y_3 dr$$

$$I_5 = \int_0^1 \lambda y_3^2 dr$$

$$I_6 = \int_c^1 2\mu (r^2\dot{y}_1^2 + 2y_1^2) dr$$

$$I_7 = \int_c^1 \mu (y_1^2 - y_3^2 - 6y_1y_3 + 2ry_1\dot{y}_3 - 2ry_3\dot{y}_3 + r^2\dot{y}_3^2) dr$$

$$I_8 = \int_0^1 \mu y_3^2 dr$$

12.

and group velocity is calculated from the formula:

$$U = \frac{(I_7 - 2I_4) + 2N^2(I_5 + /2I_8) - (\sigma a)^2 I_2}{c(I_1 + N^2 I_2)}$$

In the present study, the earth has been modelled consisting of 26 spherical layers to a depth of 1200 km. Each layer is specifies by the compressional velocity, shear velocity, density, and the layer thickness.

Partial derivatives of group velocity with respect to the layer parameters are derived and calculated from these energy integrals. Due to wide variations in the numerical values, however, they have not been used.

The fitting process was accomplished in the following manner: density in each layer was taken from published earth models (Wang, 1970; Press, 1970) and is kept unchaged since the group velocity is not very sensitive to its changes (only 10% as sensitive as shear velocity changes). If the observed Love wave dispersion is available, shear wave velocities are varied to fit the observations. In general, group velocities are most sensitive to the structure within one-third of their wave lengths. For this reasons, the fitting was proceeded from short periods to longer periods. Which corresponds from shallower structures to deeper structures. Final fitting is achieved when the differences between the observed and the calculated group velocities are less than 0.04 km/sec in the period range of 20 to 100 seconds.

Once the shear velocities and the thicknesses have been determined by the Love dispersion, compressional velocities are changed in the model to fit the Rayleigh wave dispersion data.

For those wave-paths that there are no Love wave dispersions available, the fitting was accomplished by varying both compressional velocities and shear velocities in a manner that Poisson's ratio holds.

In our study, the constant C has been set to be from .3 to .45 depend on arrival times of late signals as relating to fundemental mode waves.

VI. RESULTS AND TECTONIC IMPLICATIONS

We have selected surface wave data from a variety combinations of paths:

(1)   Those sampling various parts of the Tibetan platform only,

(2)   Those sampling various parts of the southeast China platform
only, and

(3)   Those sampling both the Tibetan and southeast China platforms.

These combinations of wave paths not only allow a study of lateral variation
of crustal structure within a tectonic element, but also provide an empirical
confirmation of using regionalization idea to explain surface wave dispersion
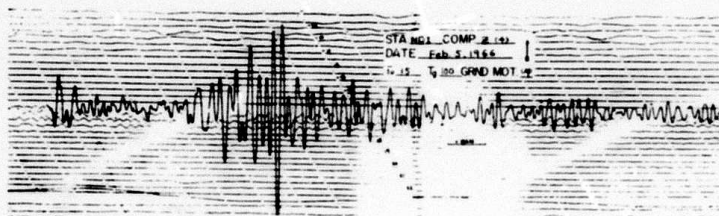data across two tectonic elements.

Nine dispersion curves are obtained in the area of Tibetan platform for
both Love and Rayleigh waves, three dispersion curves are obtained for the
southeast China area, another four dispersion curves for wave paths crossing
both these areas. The seismograms and the corresponding dispersion data are
presented in groups in Figures 4 through 11. For ease of identification, figure
numbers of the surface wave trains and dispersions curves are tabulated in
Table 2. Numerical values of the dispersion curves are given in Table 3 for
each wave path. Our dispersion plots gives the wave energy distribution
as a function of group velocity, they differ from those of Dziewonski's in
that the amplitudes are normalized with respect to the maximum amplitude values
for each frequency, but not the maximum amplitude value of the entire spectrum.
Consequently, our dispersion plots do not show the relative excitation of wave
energy at various frequencies. Yet our normalization procedure tends to amplify
the small energy in long-period range so that the dispersion can be more easily
observed. A study of these dispersion plots enables one to identify the
presence of higher modes, reflected later arrivals, and especially at the
long-period end the high background noise. Thus, these dispersion plots allow
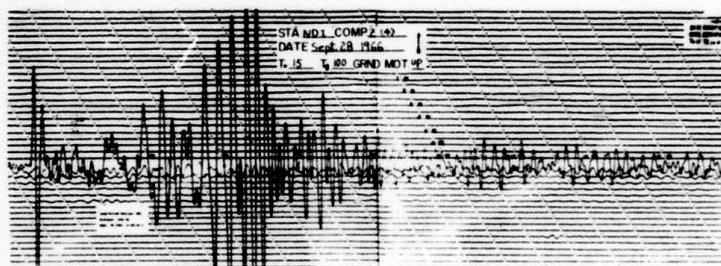
TABLE 2

Region	Wave form Figure Number	Dispersion Figure Number
Tibet	4A	5A
(S.W. China)	4B	5B
	4C	5C
	4D	5D
	6C	7C
	6D	7D
	8A	9A
	8B	9B
	10B	11B
S. E. China	6A	7A
	6B	7B
	8C	9C
Entire S. China	8D	9D
	10A	11A
	10C	11C
	10D	11D

A

B

C

D

Fig. 4

15a

Fig. 5A

LAH vertical component
February 5 1966
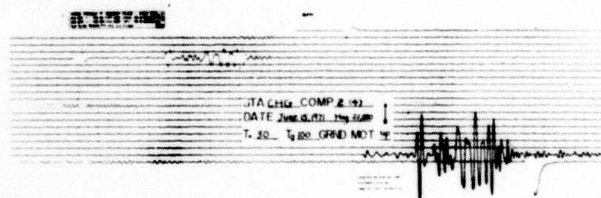
PERIOD (second)

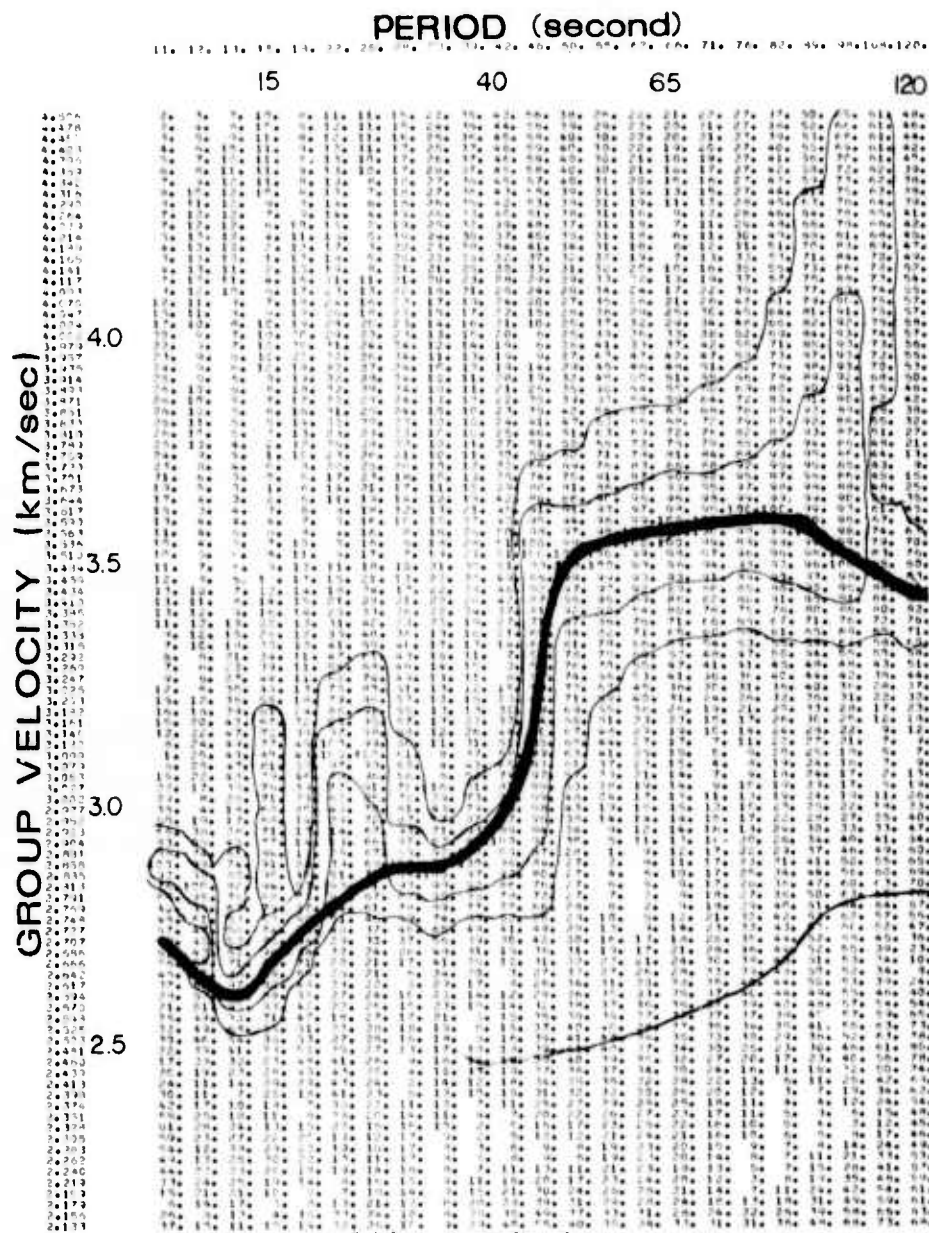NDI vertical component
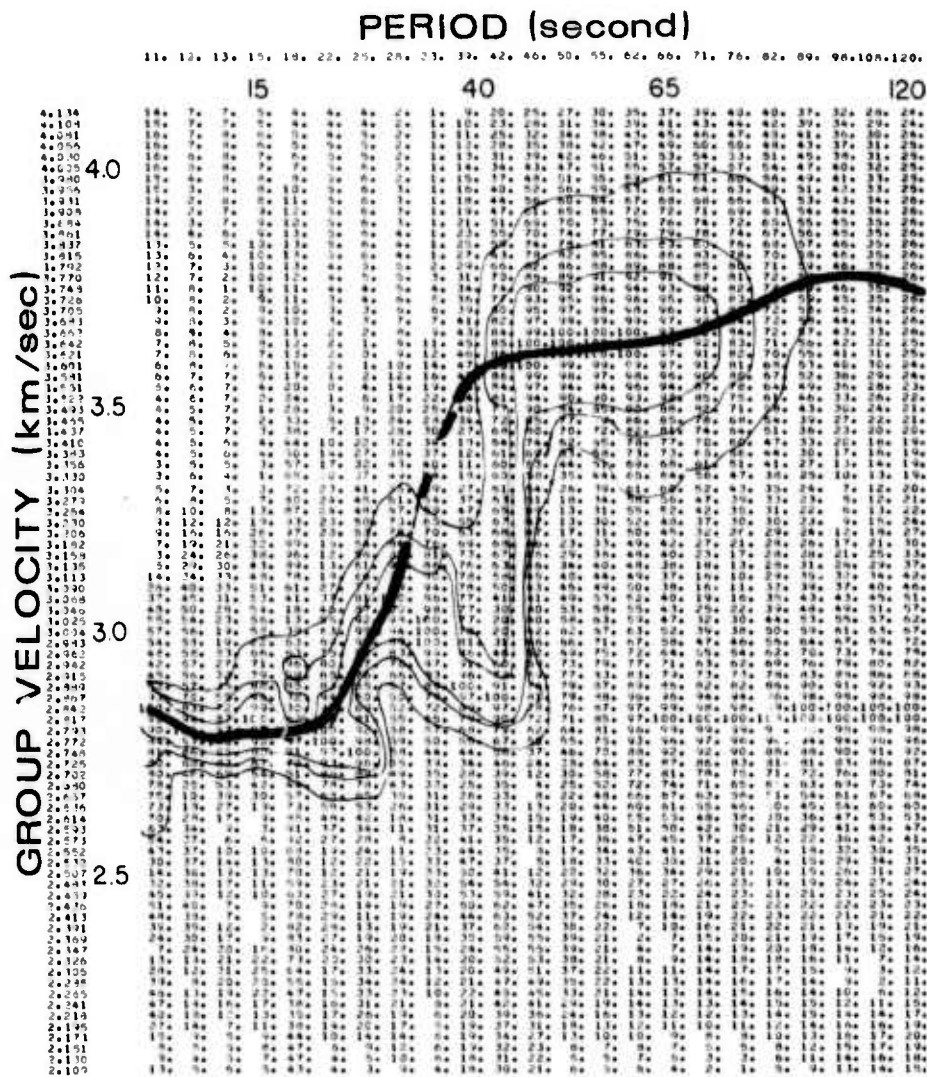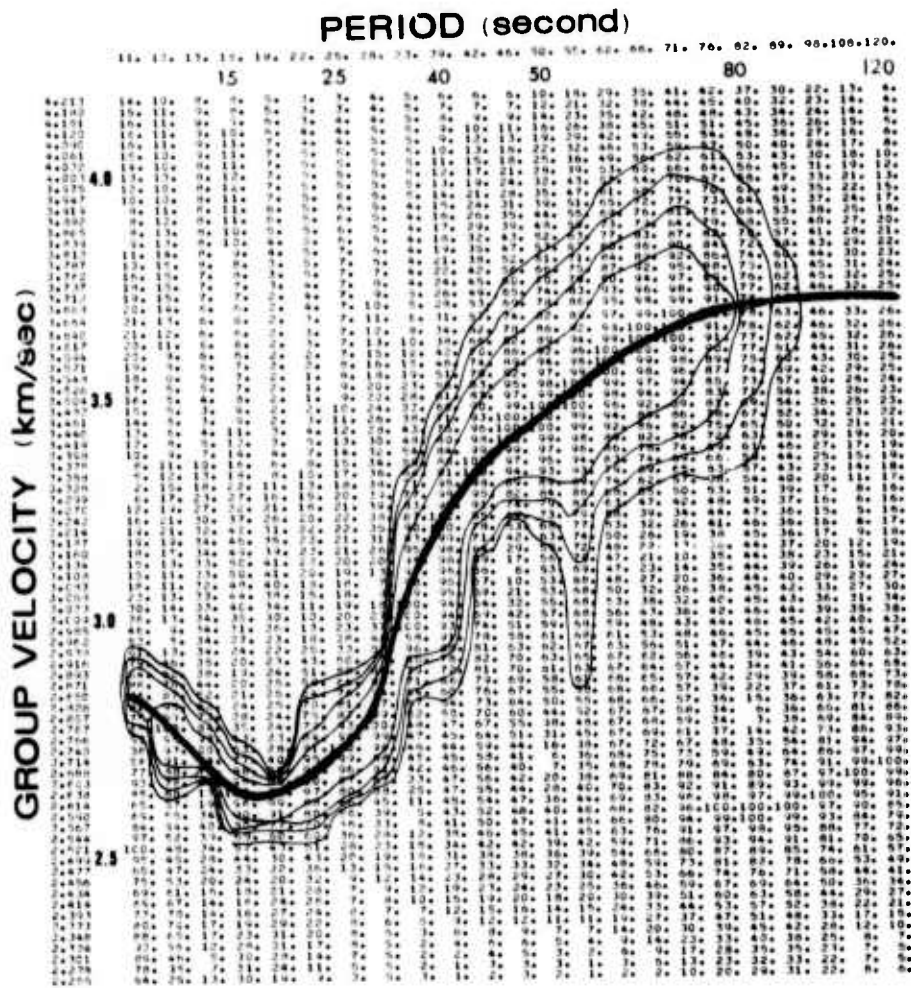February 5 1966

Fig. 5 B

NDI vertical component
September 28 1966
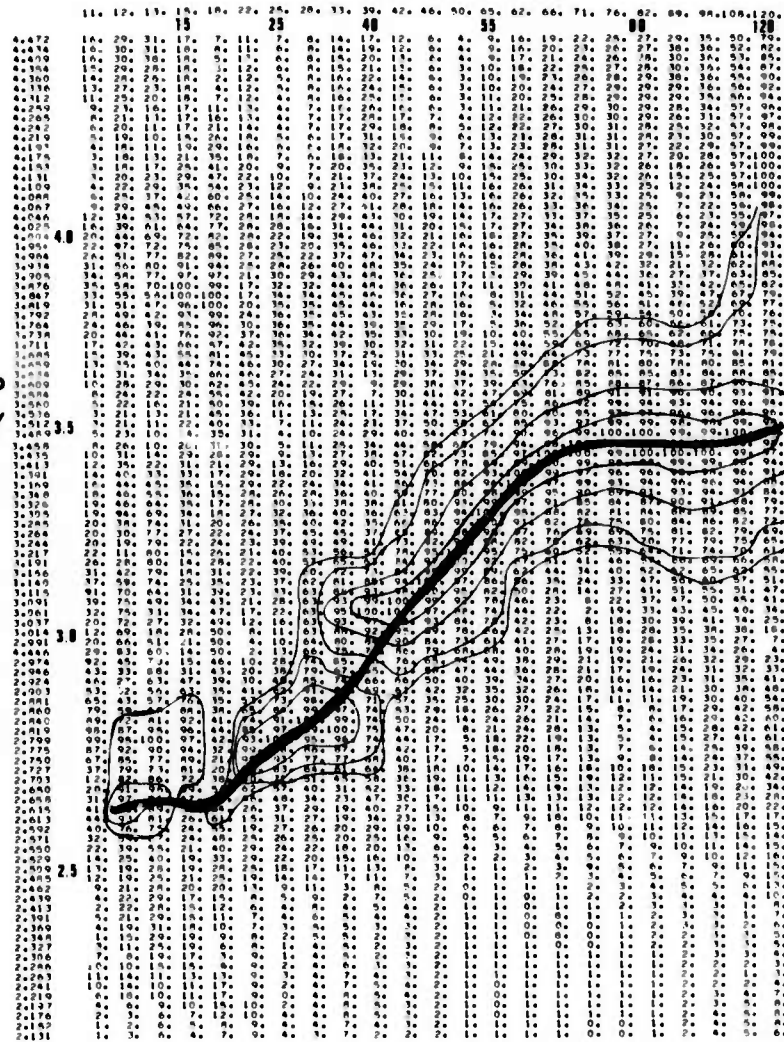
Fig. 5C

15 2

PERIOD (second)

GROUP
VELOCITY
(km/sec.)

CHG   vertical component
June 15   1971

Fig. 5 D

A

B

C

D

158

Fig. 6

ANP N.-S component
February 13 1966

Fig. 7A

ANP N-S component
February 5 1966

Fig. 7 B

15 k

PERIOD (second)

GROUP VELOCITY (km/sec)

NDI N-S component
Sept. 28 1966

Fig. 7 C

15 i

PERIOD (second)
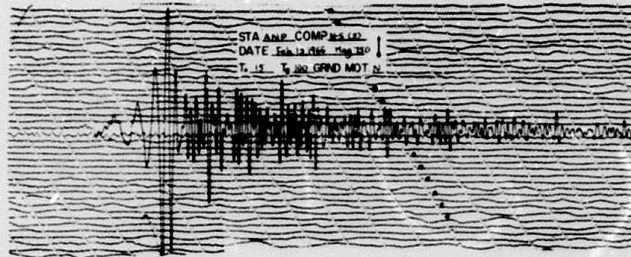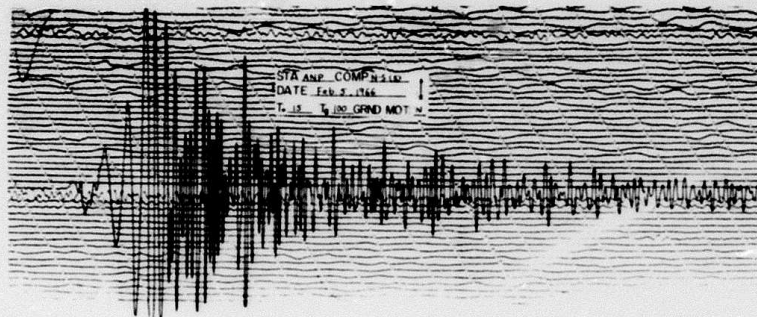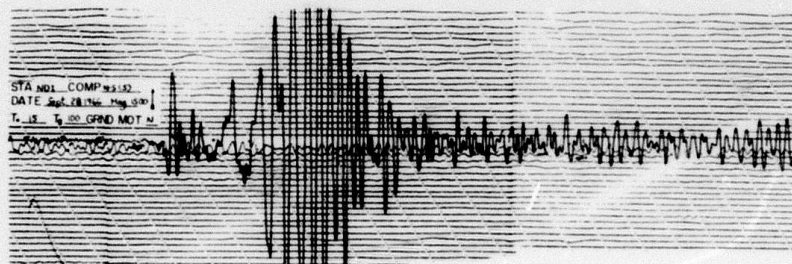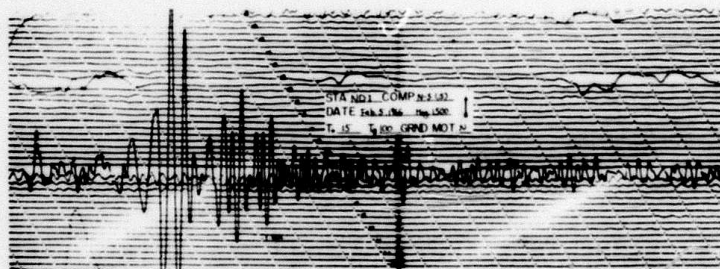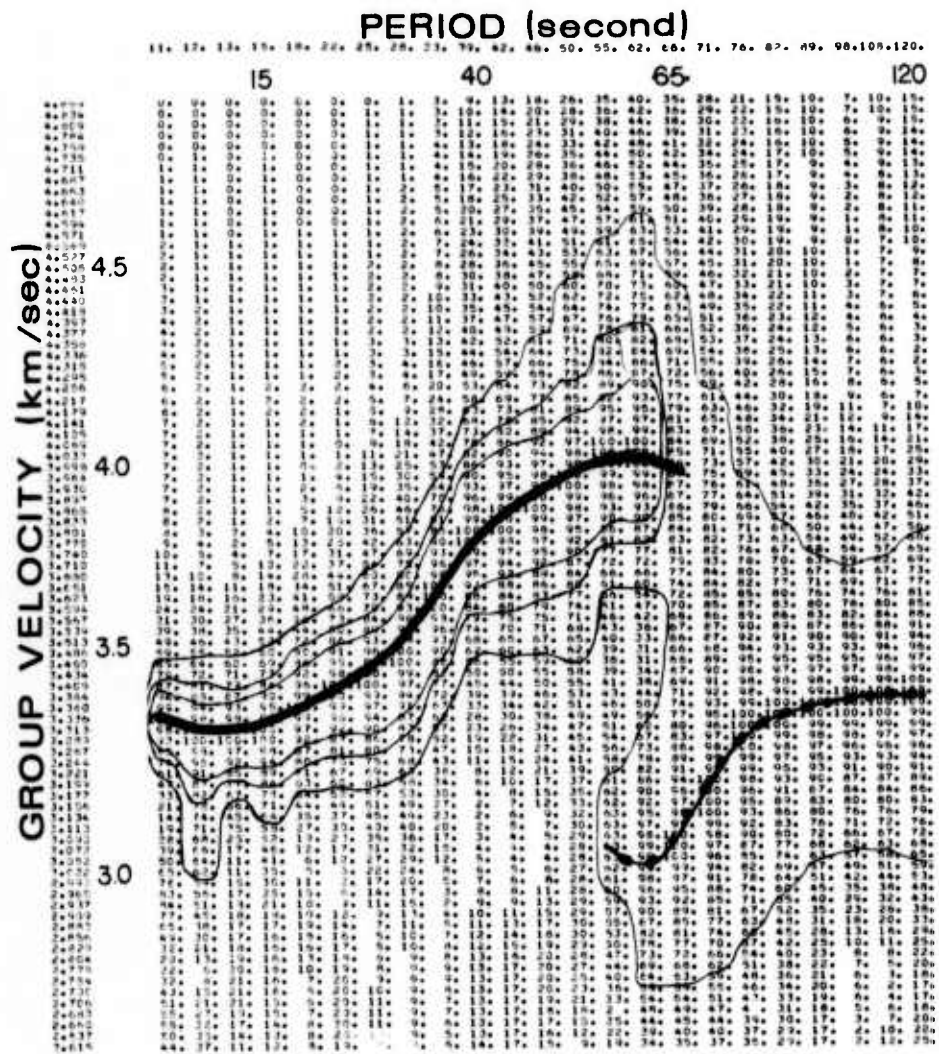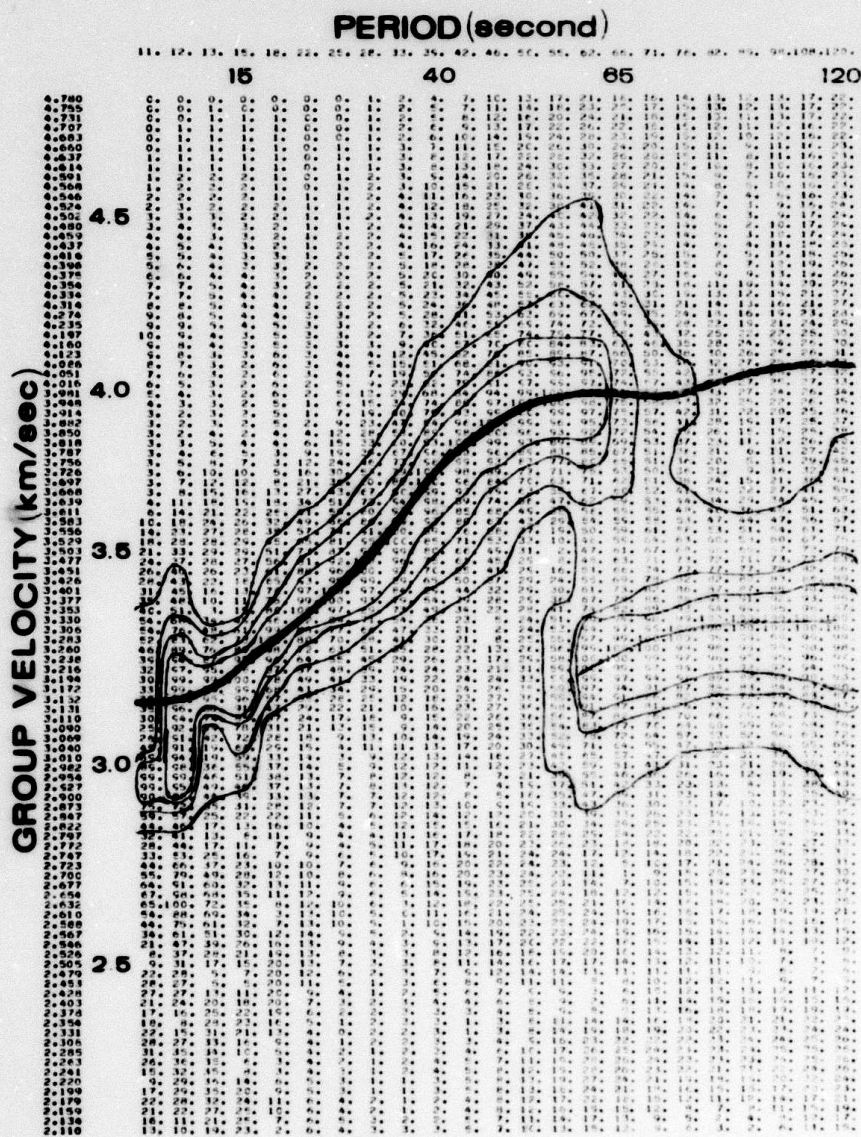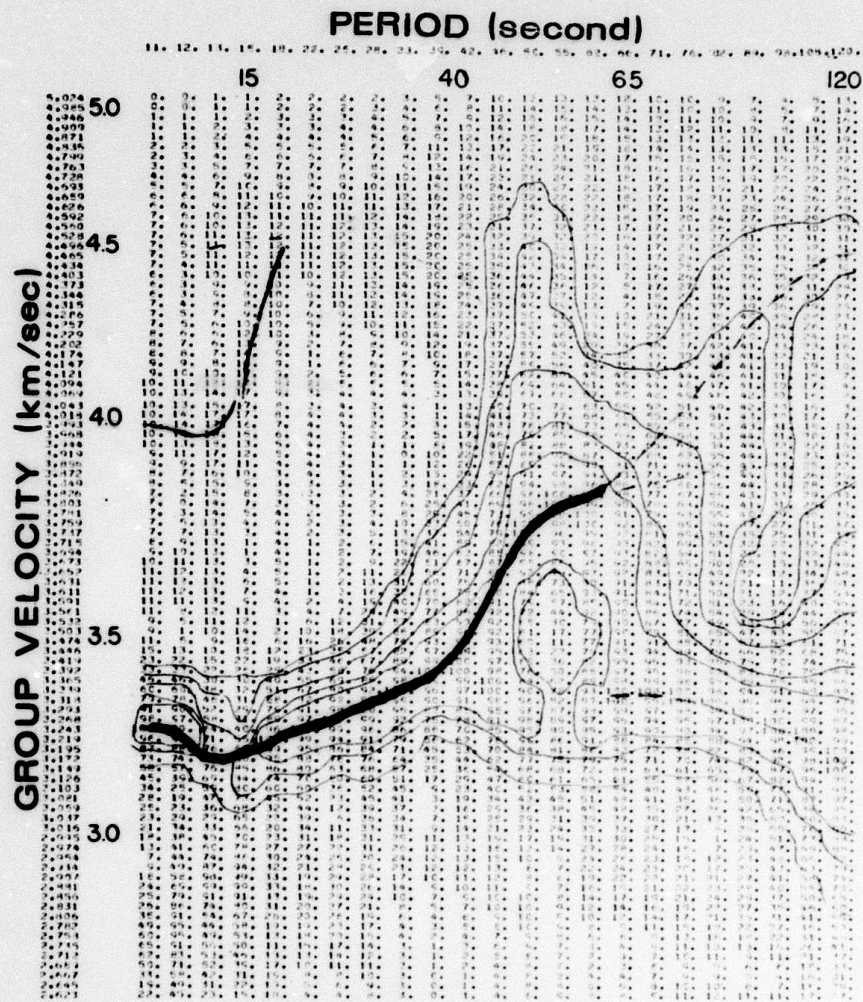
NDI N-S component
February 5 1966

Fig. 7 D

A

B

C

D

Fig. 8

15 R
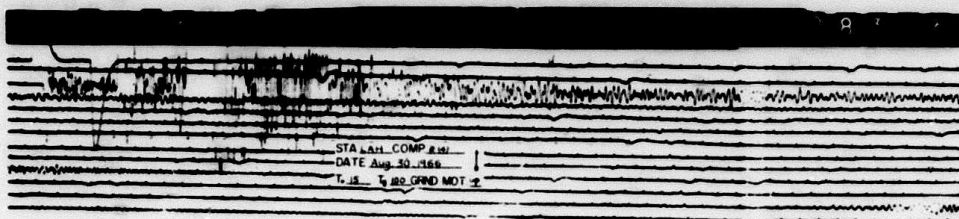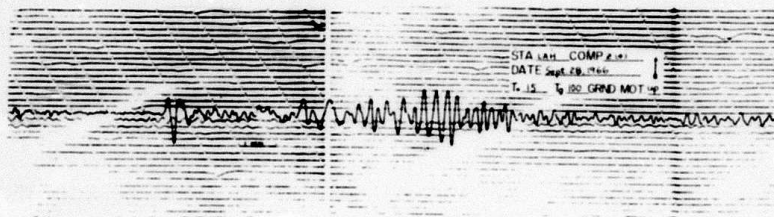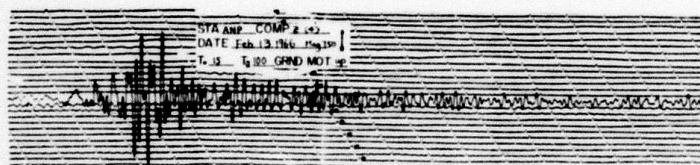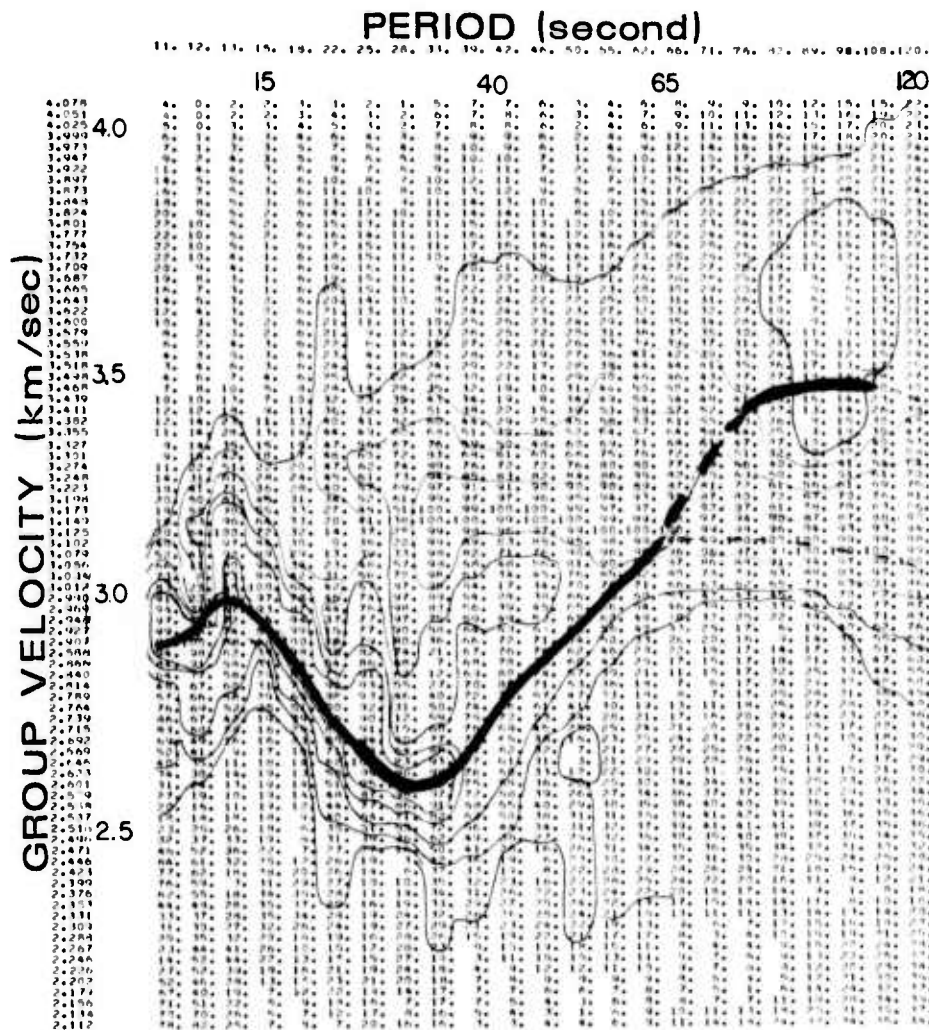
LAH vertical component
August 30 1967

Fig. 9 A

15 1

PERIOD (second)

LAH vertical component
Sept. 28 1966

Fig. 9 B

ANP vertical component
February 13 1966

Fig. 9 C

15 N

ANP vertical component
Feb. 7 1966

Fig. 9 D

A

B

C

D

Fig. 10

15 p

PERIOD (second)

ANP N-S Component
February 7 , 1966

Fig. 11 A

PERIOD (second)
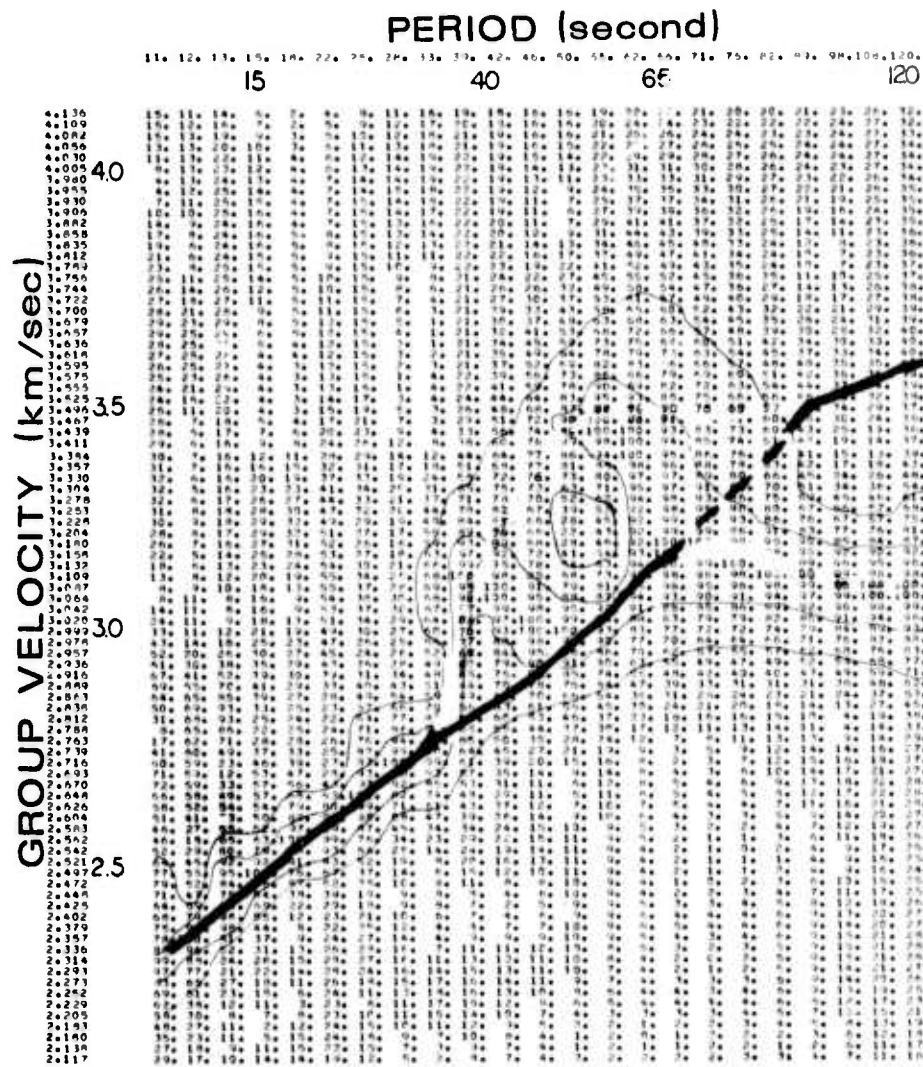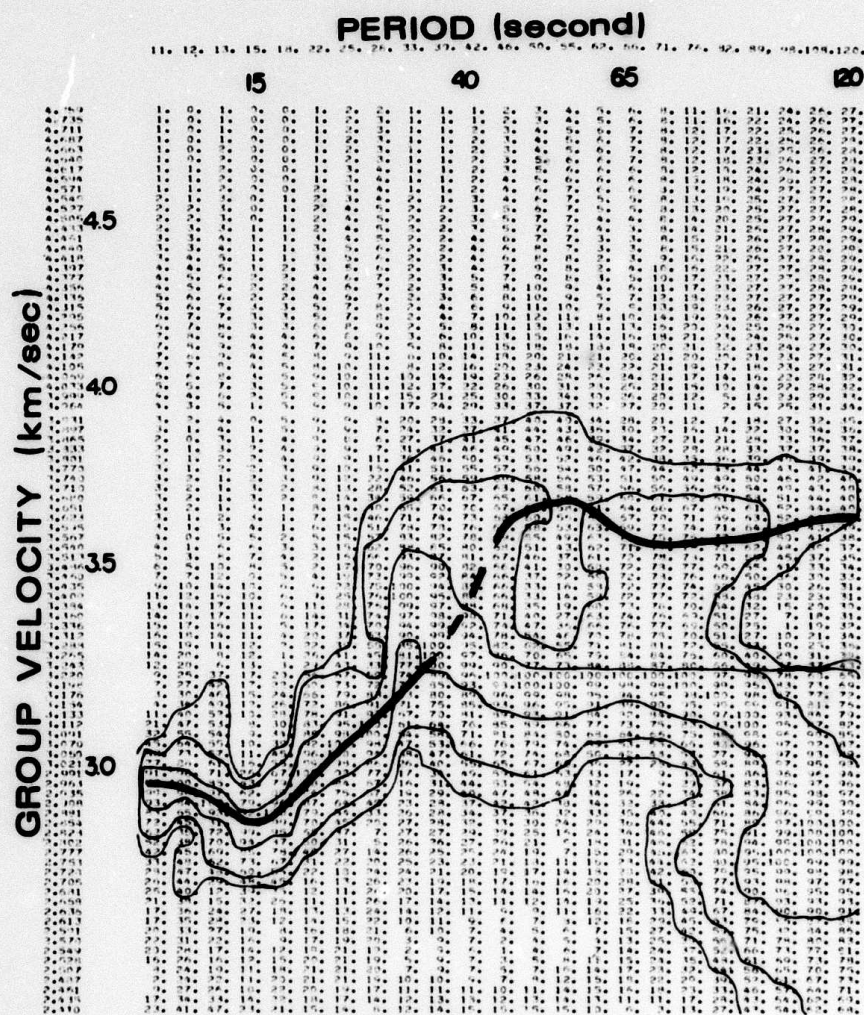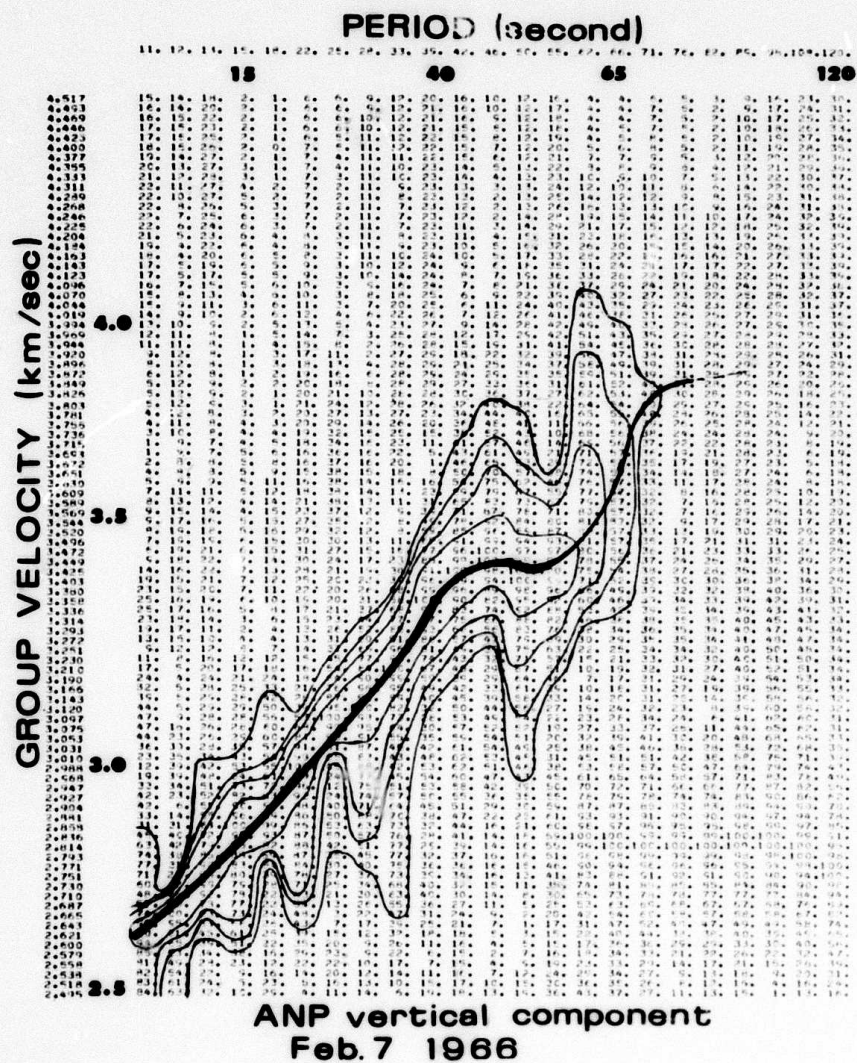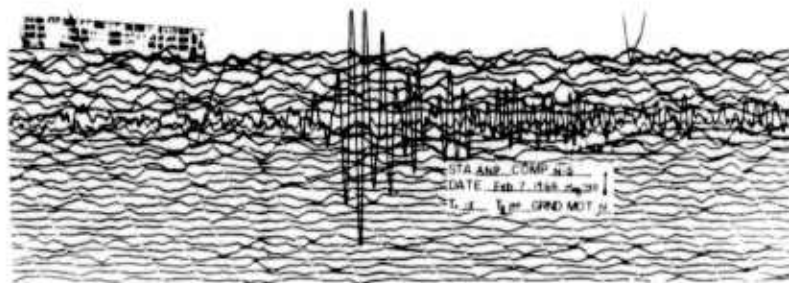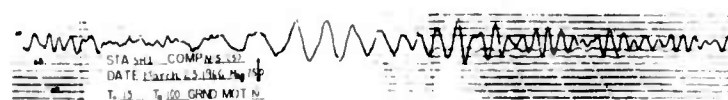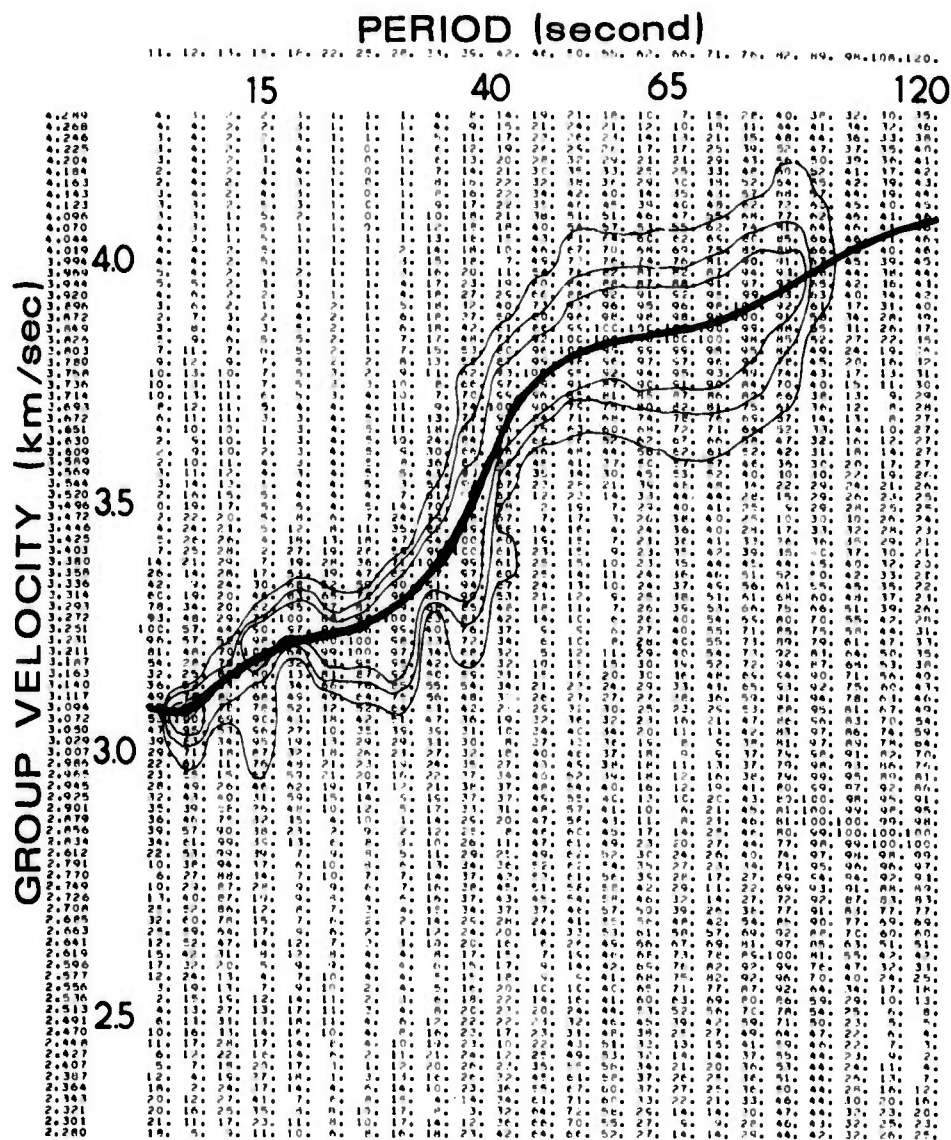
GROUP VELOCITY (km/sec)
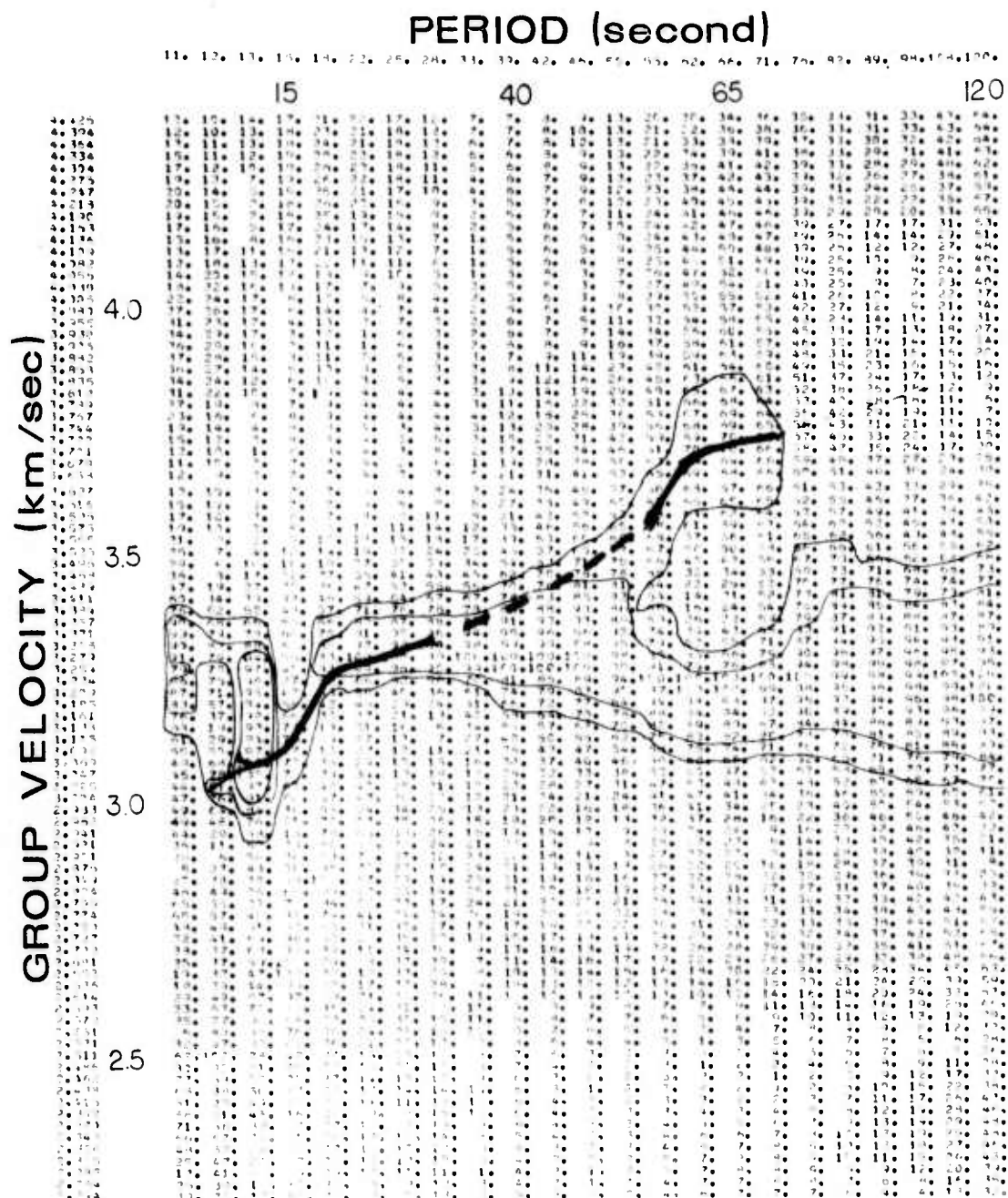
LAH N-S component
September 28 1966

Fig. 11 B

SHI N-S Component
march 23 , 1966

Fig. 11 C

LAH N-S component
March 23 1966
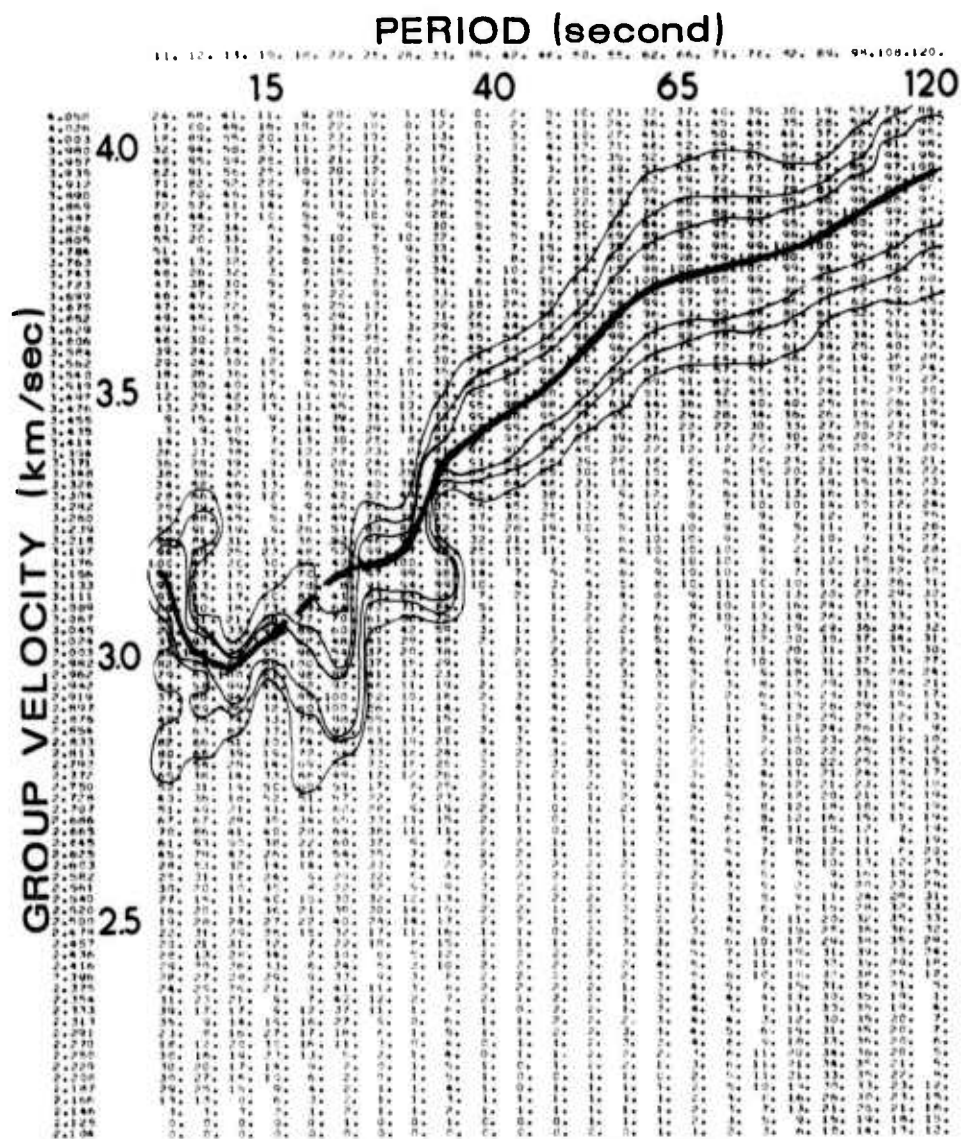
Fig. 11 D
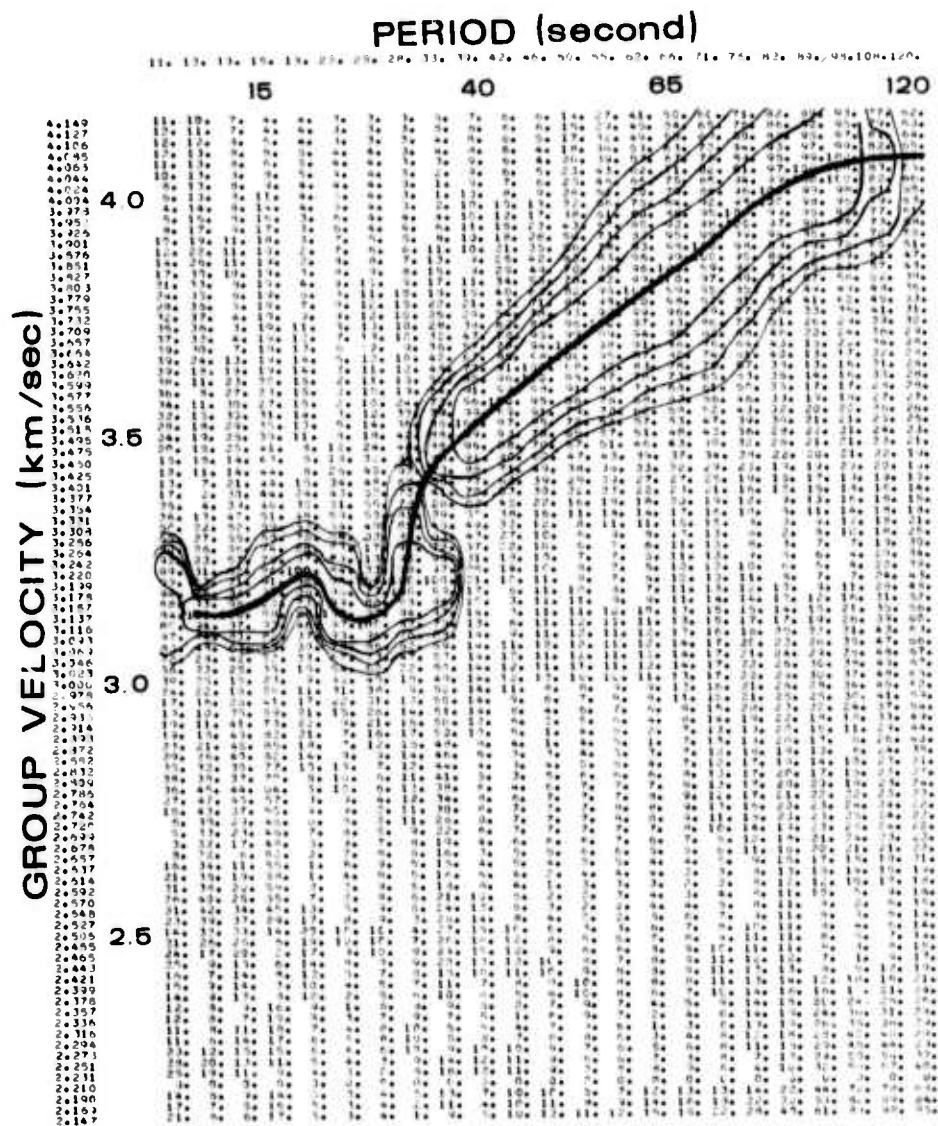
SHI   COMP 5   MARCH 23, 1966

PERIOD	GROUP VELOCITY	PERIOD	GROUP VELOCITY	PERIOD	GROUP VELOCITY
120.471	3.926	62.061	3.703	24.675	3.185
107.789	3.882	55.351	3.637	22.021	3.133
97.524	3.834	49.951	3.562	18.124	3.089
89.043	3.796	45.511	3.501	15.398	3.024
81.920	3.772	41.796	3.459	13.386	2.957
75.852	3.755	38.641	3.435	11.838	3.005
70.621	3.743	32.508	3.326	10.611	3.171
66.065	3.727	28.055	3.171		

ANP   COMP 5   FEBRUARY 7, 1966

PERIOD	GROUP VELOCITY	PERIOD	GROUP VELOCITY	PERIOD	GROUP VELOCITY
120.471	4.070	62.061	3.832	24.675	3.223
107.789	4.044	55.351	3.837	22.021	3.223
97.524	4.019	49.951	3.814	18.124	3.268
89.043	3.994	45.511	3.758	15.398	3.215
81.920	3.944	41.796	3.698	13.386	3.140
75.852	3.878	38.641	3.412	11.838	3.072
70.621	3.843	32.508	3.385	11.611	3.052
66.065	3.832	28.055	3.272		

TABLE THREE-GROUP VELOCITY DATA

PERIOD	GROUP VELOCITY	PERIOD	GROUP VELOCITY	PERIOD	GROUP VELOCITY
107.789	4.069	55.351	3.981	22.021	3.397
97.524	4.069	49.951	3.930	18.124	3.360
89.043	4.069	45.511	3.881	15.398	3.313
81.920	4.069	41.796	3.817	13.386	3.301
75.852	4.053	38.641	3.755	11.838	3.301
70.621	4.033	32.508	3.608	10.611	3.324
66.065	4.033	28.055	3.486		
62:061	4.016	24.675	3.422		

TABLE THREE (CONTINUED)

ANP COMP 4 FEBRUARY 13, 1966

PERIOD	GROUP VELOCITY	PERIOD	GROUP VELOCITY	PERIOD	GROUP VELOCITY
120.471	3.710	62.061	3.623	24.675	3.060
107.789	3.651	55.351	3.680	22.021	3.001
97.524	3.623	49.951	3.651	18.124	2.872
89.043	3.593	45.511	3.595	15.398	2.837
81.920	3.540	41.796	3.460	13.386	2.917
75.852	3.513	38.641	3.288	11.838	2.963
70.621	3.513	32.508	3.198	10.611	2.944
66.065	3.567	28.055	3.101		

ANP COMP 5 FEBRUARY 5, 1966

PERIOD	GROUP VELOCITY	PERIOD	GROUP VELOCITY	PERIOD	GROUP VELOCITY
107.789	4.026	62.061	3.981	24.675	3.401
97.524	4.070	55.351	3.964	22.021	3.353
89.043	4.051	49.951	3.931	18.124	3.283
81.920	4.016	45.511	3.866	15.398	3.183
75.852	3.921	41.796	3.787	13.386	3.183
70.621	3.981	38.641	3.697	11.838	3.152
66.065	3.981	32.508	3.543	10.611	2.945
		28.055	3.451		

ANP COMP 4 FEBRUARY 5, 1966

PERIOD	GROUP VELOCITY	PERIOD	GROUP VELOCITY	PERIOD	GROUP VELOCITY
120.471	3.565	49.951	3.737	18.124	2.899
107.789	3.565	45.511	3.678	15.398	2.899
97.524	3.565	41.796	3.660	13.386	2.982
66.065	3.760	38.641	3.510	11.838	3.001
62.061	3.768	24.675	2.982	10.611	2.963
55.351	3.760	22.021	2.917		

TABLE THREE (CONTINUED)

LAH   August 30, 1967

Period	Velocity	Period	Velocity	Period	Velocity
120.471	3.439	62.061	3.034	24.675	2.640
107.789	3.468	55.351	3.990	22.021	2.770
97.524	3.468	49.951	2.927	18.124	2.913
89.043	3.468	45.511	2.866	15.398	3.012
81.920	3.439	41.796	2.814	13.386	3.117
75.852	3.411	38.641	2.692	11.838	2.900
70.621	3.274	32.508	2.623	10.611	2.913
66.065	3.149	28.055	2.601		

NDI   COMP 4   February 5, 1966

Period	Velocity	Period	Velocity	Period	Velocity
120.471	3.770	62.061	3.642	24.675	2.983
107.789	3.792	55.351	3.642	22.021	2.793
97.524	3.792	49.951	3.642	18.124	2.778
89.043	3.748	45.511	3.621	15.398	2.823
81.920	3.726	41.796	3.601	13.386	2.778
75.852	3.683	38.641	3.581	11.838	2.793
70.621	3.662	32.508	3.291	10.611	2.835
66.065	3.642	28.055	3.061		

CHG   COMP 4   June 15, 1971

Period	Velocity	Period	Velocity	Period	Velocity
107.789	3.473	55.351	3.292	22.021	2.765
97.524	3.450	49.951	3.211	18.124	2.700
89.043	3.450	45.511	3.128	15.398	2.620
81.920	3.458	41.796	3.079	13.386	2.630
75.852	3.473	38.641	3.073	11.838	2.640
70.621	3.450	32.508	2.930	10.611	2.809
66.065	3.420	28.055	2.835		
62.061	3.384	24.675	2.794		

TABLE THREE (CONTINUED)

LAH   COMP 4   September 28, 1966
Rayleigh Wave

Period	Velocity	Period	Velocity	Period	Velocity
120.471	3.575	62.061	3.087	24.675	2.693
107.789	3.555	55.351	3.042	22.021	2.602
97.524	3.525	49.951	2.978	18.124	2.583
89.043	3.439	45.511	2.916	15.398	2.542
82.000	3.357	41.796	2.863	13.386	2.458
75.852	3.325	38.641	2.812	11.838	2.562
70.621	3.204	32.508	2.763	10.611	2.610
66.065	3.180	28.055	2.722		

NDI   COMP 5   September 28, 1966

Period	Velocity	Period	Velocity	Period	Velocity
120.471	3.826	55.351	3.670	22.021	3.051
107.789	3.846	49.951	3.644	18.124	2.929
97.524	3.846	45.511	3.510	15.398	2.831
89.043	3.819	41.796	3.315	13.386	2.776
81.920	3.794	38.641	3.257	11.838	2.756
75.852	3.768	32.508	3.229		
66.065	3.748	28.055	3.171		
62.061	3.718	24.675	3.093		

LAH   COMP 4   February 5, 1966

Period	Velocity	Period	Velocity	Period	Velocity
81.920	3.626	45.511	3.060	22.021	2.769
75.852	3.590	41.796	2.934	18.124	2.743
70.621	3.572	38.641	2.875	15.398	2.671
66.065	3.572	32.508	2.830	13.386	2.17
62.061	3.554	28.055	2.881		
55.351	3.434	24.675	2.813		

TABLE THREE (CONTINUED)

dispersion data to be extracted from complicated surface wave trains where the peak-and-through method fails.

Group arrivals in the two-dimensional dispersion plots are determined by the following criteria:

1.   Below periods of 60 sec., a few group arrivals are chosen on the basis that they are local amplitude maxima and that these maxima are consistent with values obtained by the peak-and-through method.

2.   Local amplitude maxima that can be connected to form a smooth curve in the group velocity-period space are taken to be the correct group arrivals.

3.   For period regions where no local amplitude maxima can be found to provide a smooth continuity of the dispersion curve, dashed lines are drawn to give average group arrivals.

The group velocity dispersion results are discribed by geographical regions in the following:

I Tibetan Platform

Group velocities in this area are surprisingly low, with the lowest value being 2.5 km/sec for Rayleigh waves and 2.8 km/sec for Love waves. These values are among the lowest that have every been observed over the earth's surface. It is interesting to compare the dispersion data of this area with the generalized dispersion curve of a typical continent (Figure 12), it is clear that this group velocity anomaly extends deep into the upper mouth. A finer comparison is given in Figure 13, where the Tibetan dispersion data is presented together with dispersion curves for the gutenberg model and for the Canadian Shield model. This group velocity anomaly is almost certainly due to a thick crust which may be twice as the normal crustal thickness and cause the low crustal velocity to exist down to the upper mantle region. The crustal thickness is by no means uniform throughout the Tibetan platform. In fact, the area where the Himalayas reaching the greatest heights does not correspond to the region of thickest crust. Surface
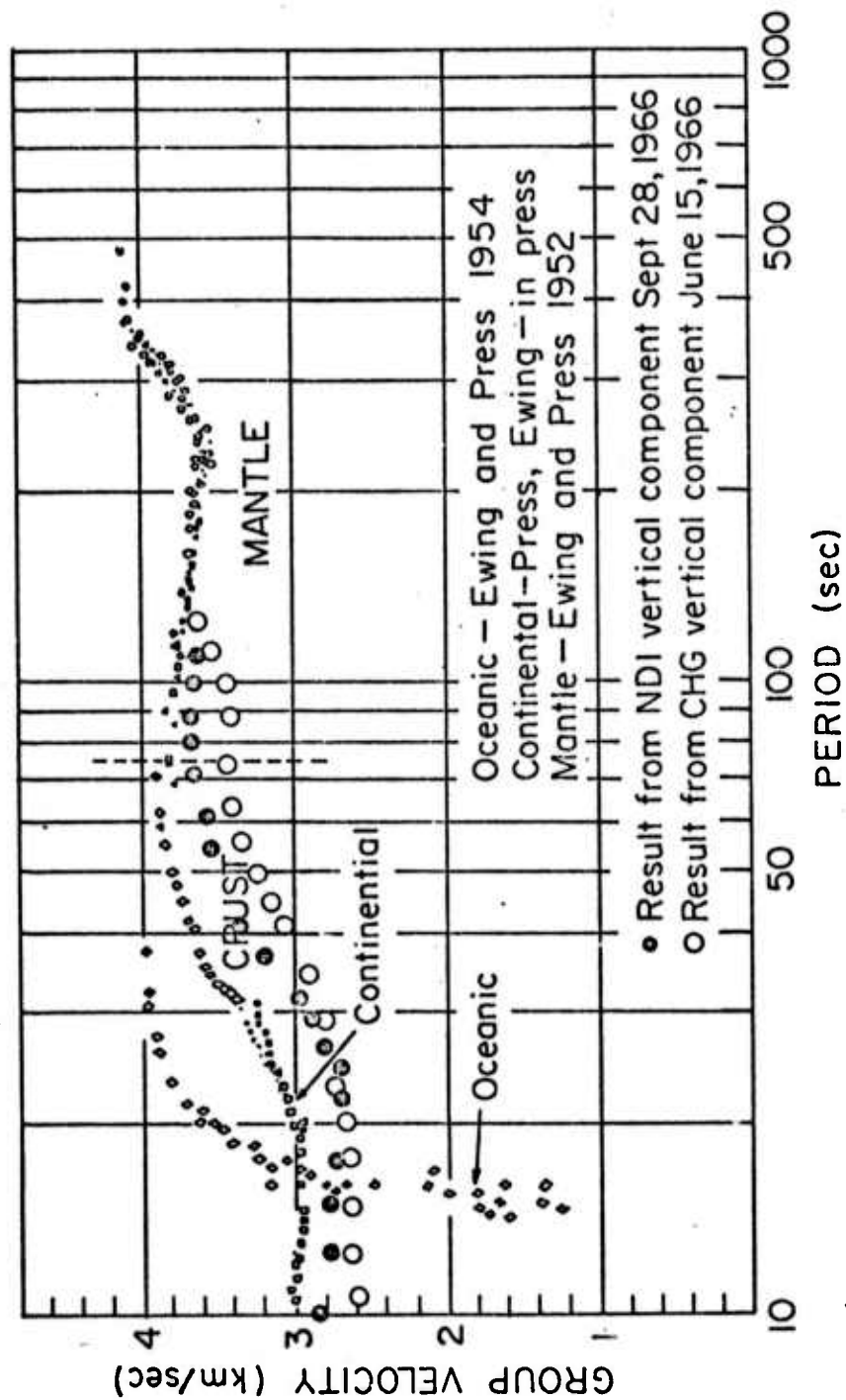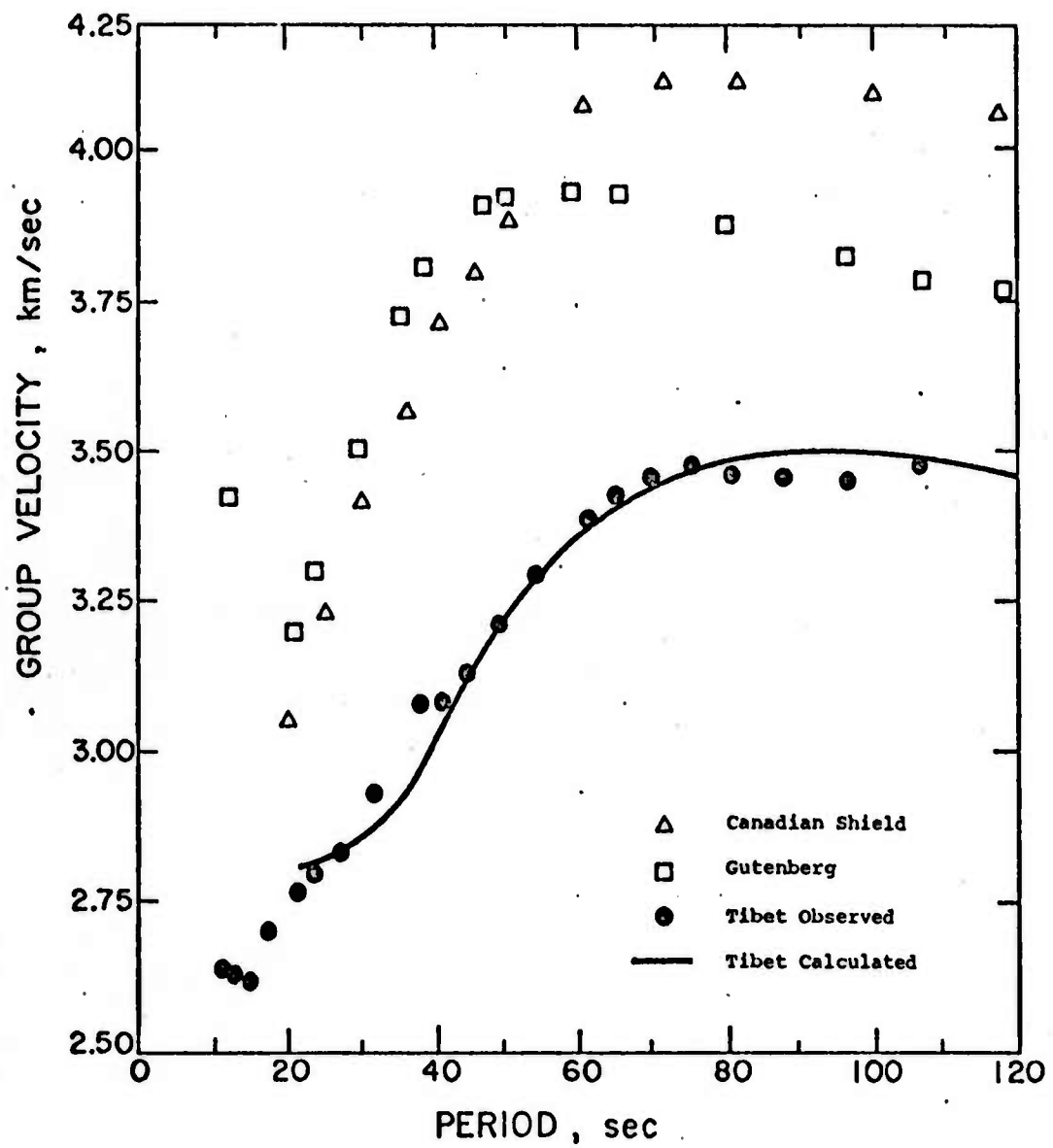
21.

FIGURE 12

RAYLEIGH WAVE DISPERSION

FIGURE 13

23.

waves passing through four regions of Tibet have their dispersion curves
plotted in Figure 14 which shows a steady decrease of group velocity from the
south toward the north, indicating a northern-thickening of the crust in the
Tibetan platform.

Theoretical dispersion curves were computed for numerous earth models.
The two models giving the best fit to the dispersion data of southern and
northern Tibet are presented in Figure 15 as T_1 and T_2 respectively. Shear
wave velocities from the Gutenberg and Canadian shield models are also plotted
in the same figure for comparasion. The important findings are:

1. An unusually thick crust about 70 km or more in the Tibetan platform
   as indicated by the velocity increase from crustal 3.8 km/sec to
   upper mantle 4.3 km/sec.

2. A thinner lid at the top of the mantle,

3. A lower velocity in the upper mantle low velocity zone, and

4. Lateral inhomogeneity in terms of crustal thickness and/or
   velocity variation exists. For several paths (NDI and CHG)
   the low group velocity in the short-period end reflects the
   existence of thick surface sediments.

II. Southeast China

Figures 6A, 6B, and 8C give the surface wave forms used, and Figures 7A, 7B,
and 9C give the corresponding dispersion curves. It is immediately recognized
that the dispersion curves are quite similar to that generated by the Gutenberg
earth model (Figure 16) except that our group velocity is consistently lower.
The resulting fit to our data gives an earth model similar in shape to the
Gutenberg's continental model with an overall shift in velocity to the lower
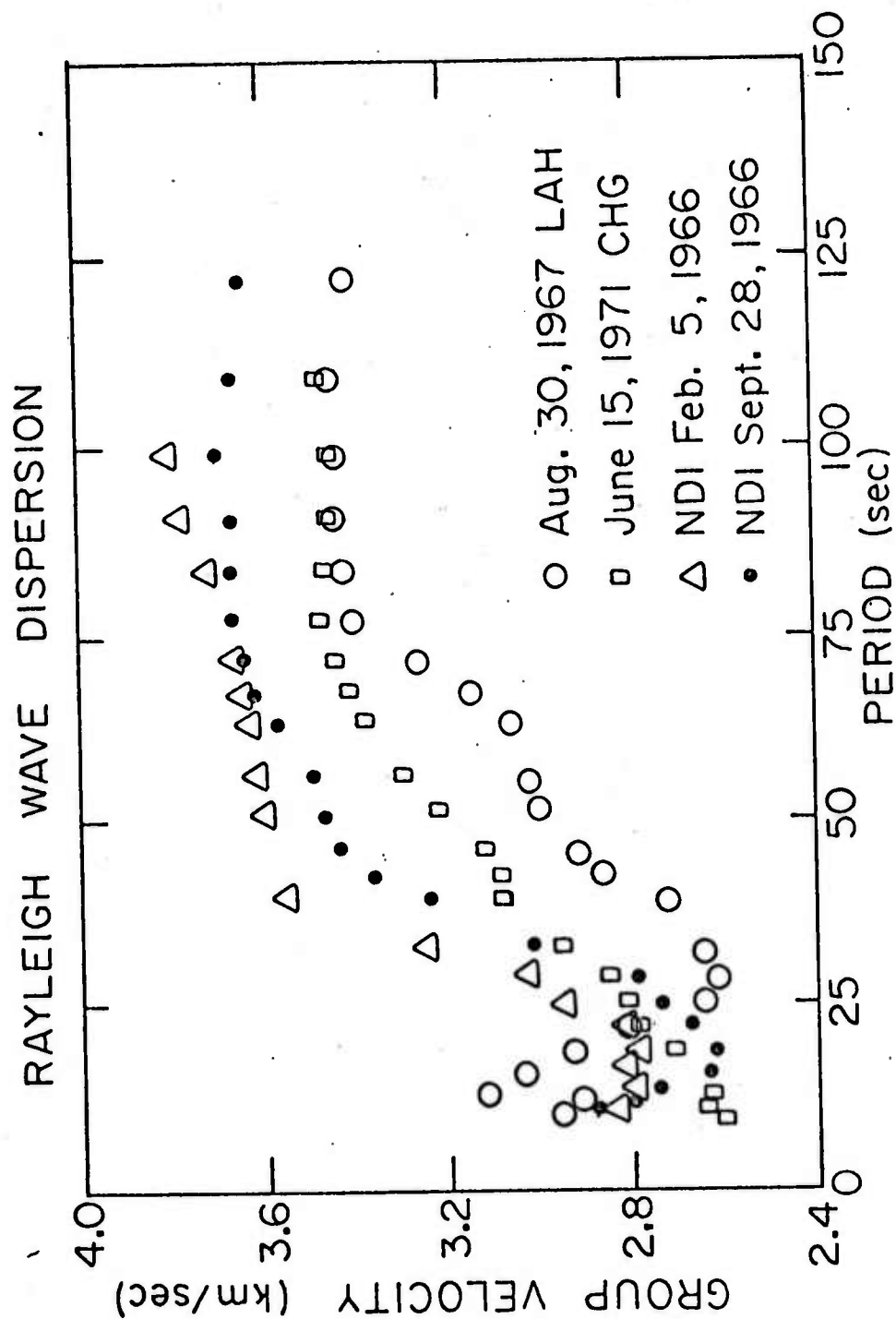side(figure 17). However, in the Southeast China there seems to be no doubt

RAYLEIGH WAVE DISPERSION

FIGURE 14

FIGURE 15

SHEAR VELOCITY , km/sec

DEPTH , km

C

G

SE

H	a	β	ρ
12	5.00	3.10	2.74
25	6.00	3.65	3.00
12	8.10	4.45	3.32
10	8.05	4.42	3.34
10	8.00	4.37	3.35
55	7.80	4.30	3.38
25	7.90	4.35	3.41
100	8.00	4.40	3.46

SE: Southeast China

G : Gutenberg
C : Canadian Shield

FIGURE 16

27.

GROUP VELOCITY (km/sec)

LOVE WAVE DISPERSION

O Gutenberg
● Result of N-S comp ANP
   Feb. 5, 1966
Model fit

PERIOD (sec)
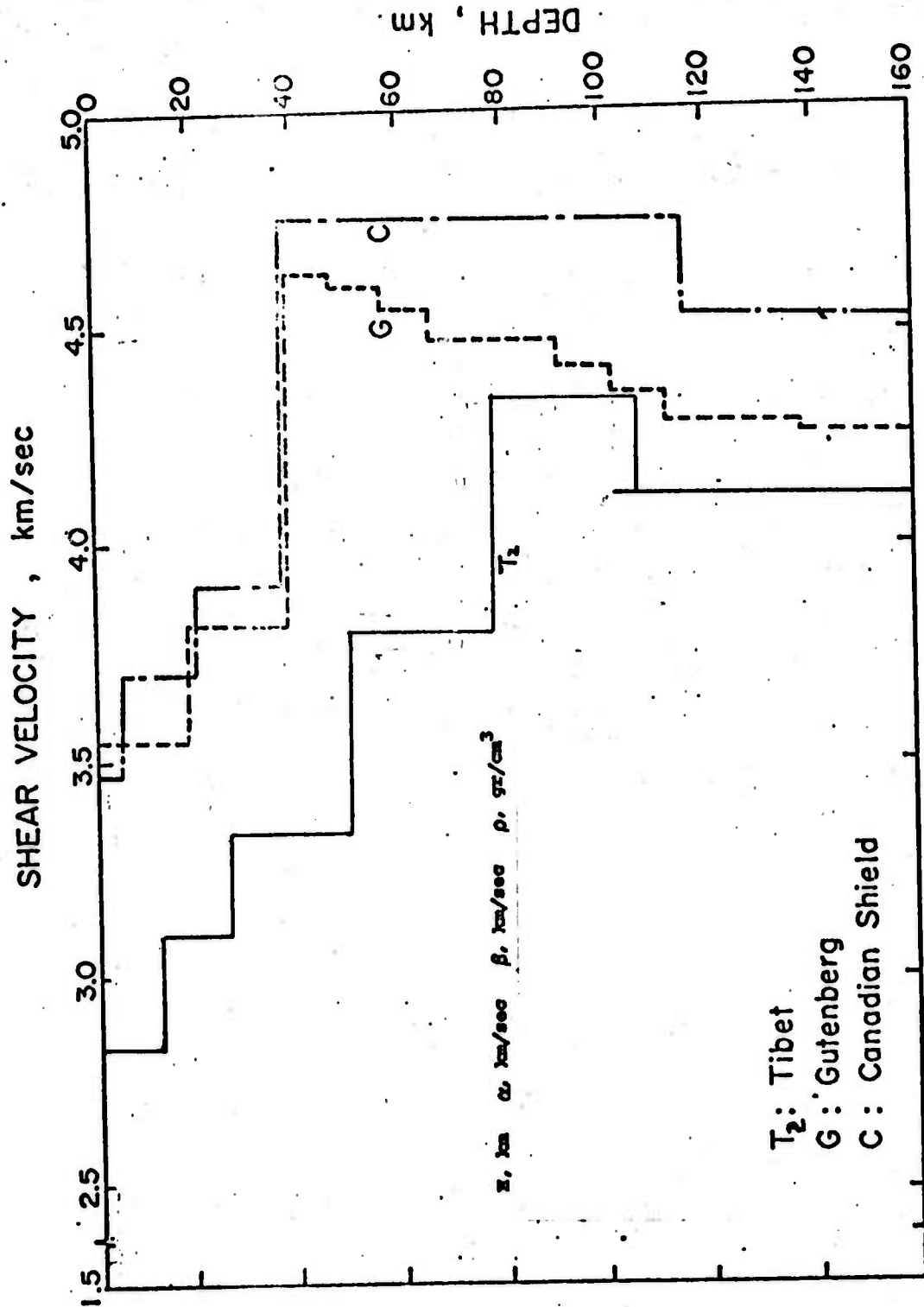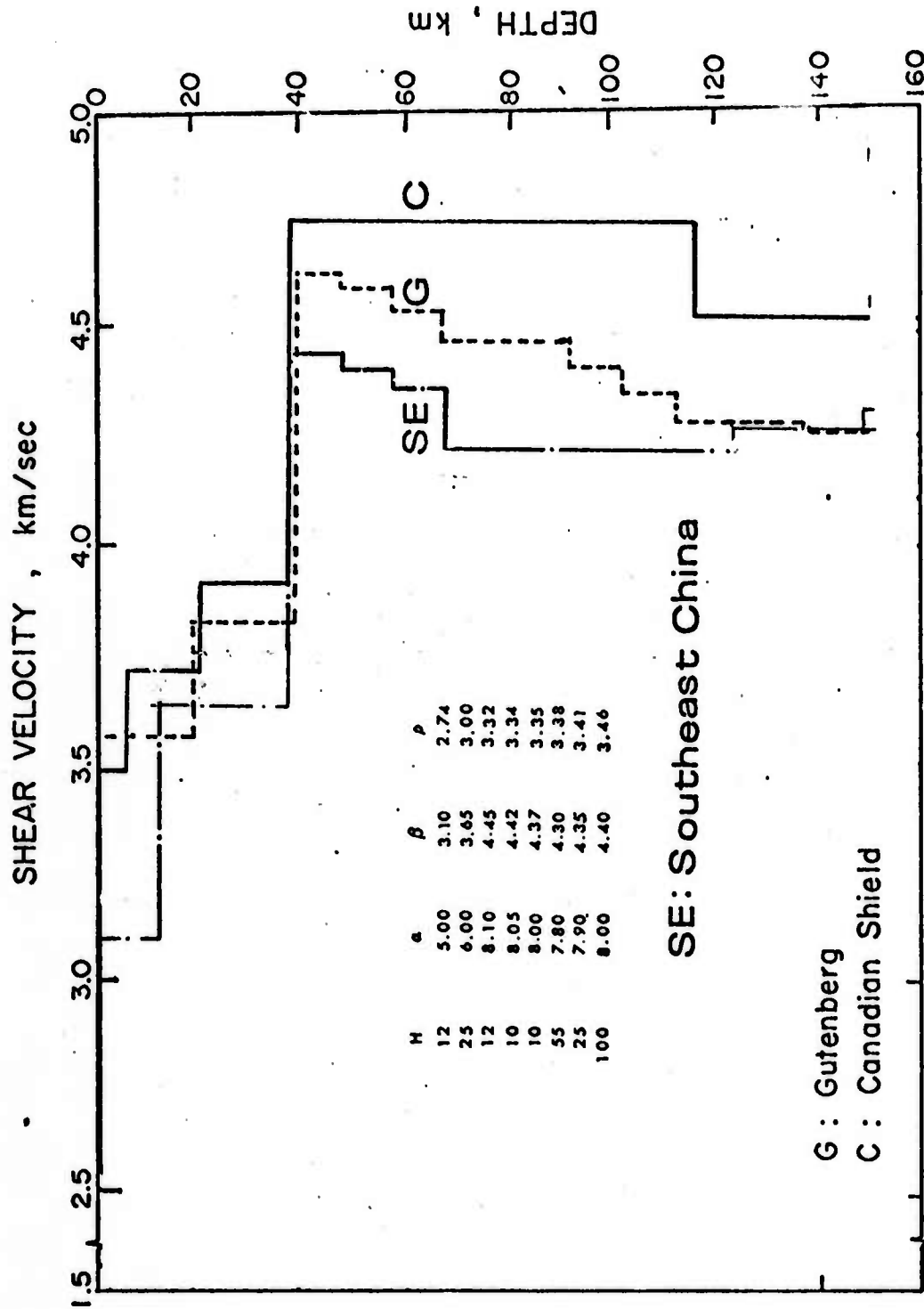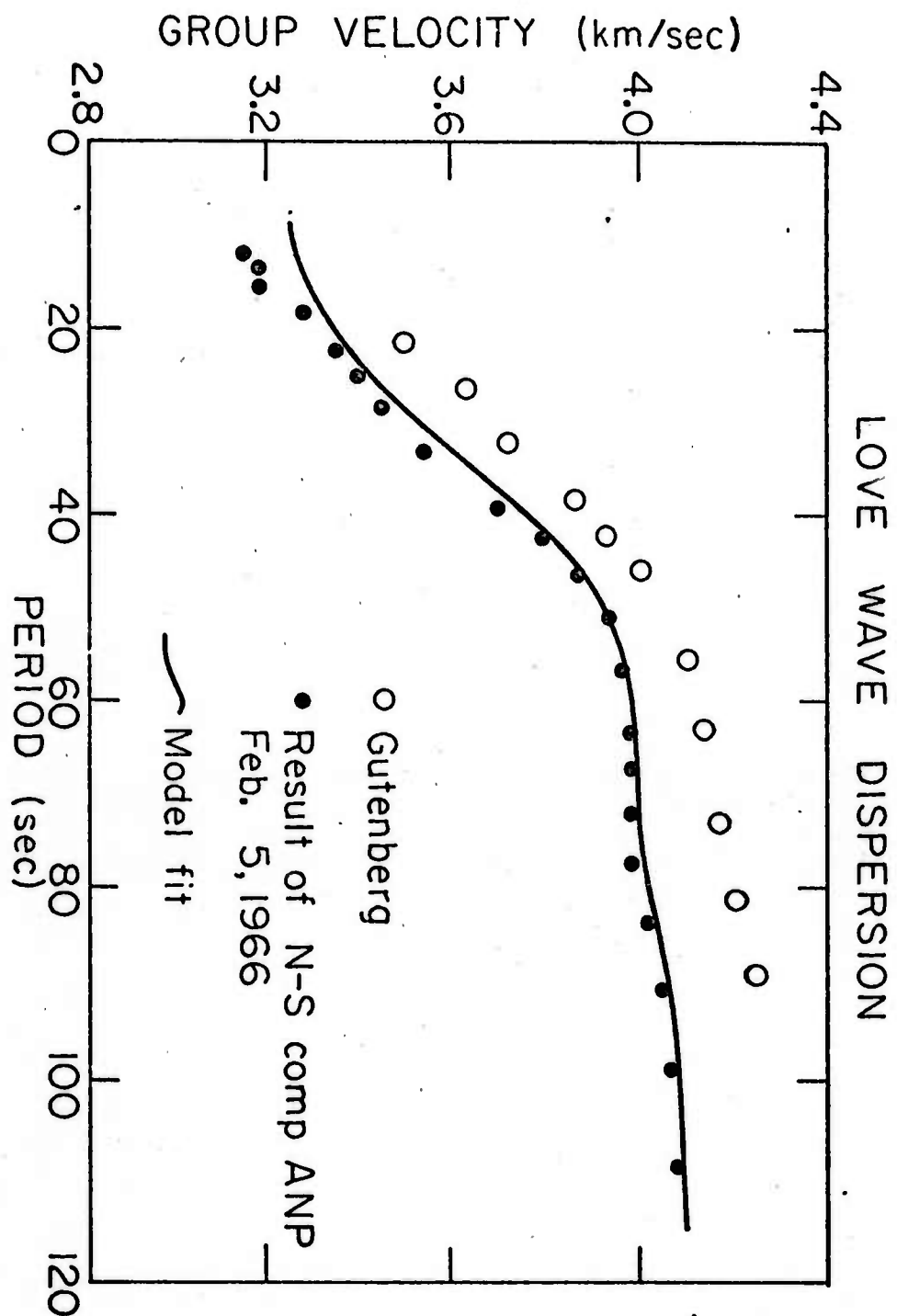
Figure 17

F 17

28.

that the crust has a normal thickness. It is interesting to find two major regions adjacent to each other as Tibet and Southwest and yet their crustal thickness differ almost by a factor of two. The drastic change in average elevation between these two regions gives the surface manifestations of the underlying tectonic differences. Moreover, the 105°E Longitude, which separates these two regions, is a major tectonic line along which there occurred great earthquakes throughout China's history. In view of the above observations, it is clear that the 105°E Longitude in South China is most likely an active plate boundary which bounds the eastern rim of the north-advancing Indian plate.

III Test of Regionalization in Surface Wave Dispersion

When surface wave travels over long great-circle path, sometime more than one crustal plate may be traversed. The resulting group velocity would have contributions from all traversed plates. In the absence of theoretical proof, it has been assumed that the resulting group velocity is the path-length weighted mean of the group velocities corresponding to each single plate. This is known as the idea of regionalization and has been used to delineate the crustal structure of single plate (or geological province) from dispersion data derived from mixed-path surface waves (Anderson and Toksoz, 1966; Kanamori, 1970; Hamada, 1972; and Wu, 1973). However, it would be desirable to seek at least an empirical confirmation to the idea of regionalization. In our study, the unique geometrical set up has made possible such an empirical test: i.g., the juxtaposition of the two plates (Tibet and Southeast China platforms) of distinct crustal thicknesses and the availability of large earthquakes (as energy sources) in Taiwan region, along the 105°E Longitude, and in West Pakistan. This set up has provided various combinations of surface wave paths:

A.   over the Tibetan platform only

B.   over the Southeast China platform only, and

C.   over both platforms.
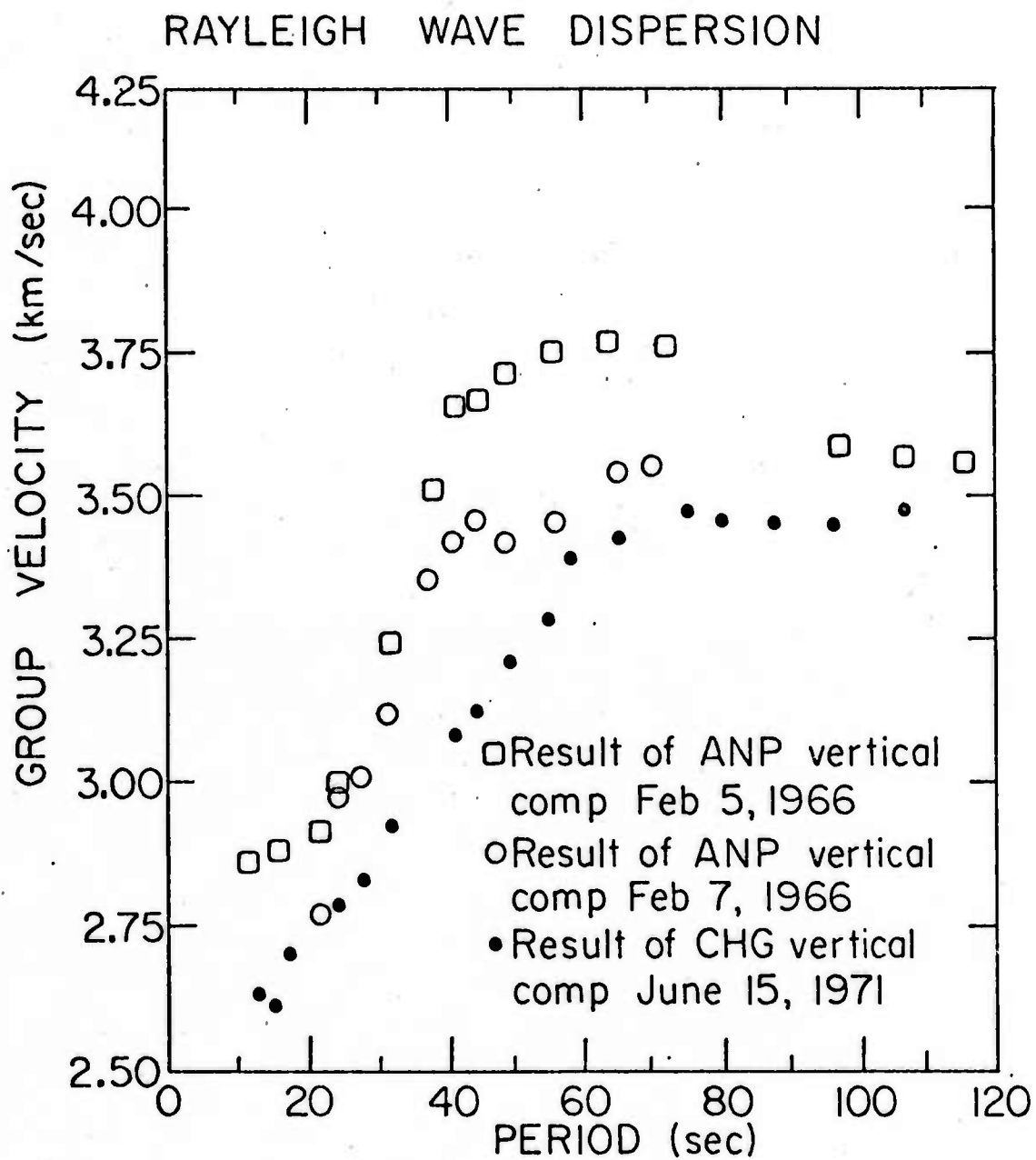
RAYLEIGH WAVE DISPERSION

FIGURE 18

LOVE WAVE DISPERSION

Result of N-S comp ANP
Feb. 5, 1966

Result of N-S comp LAH
March 23, 1966

Result of N-S comp NDJ
Sept. 28, 1966

PERIOD (sec)

GROUP VELOCITY (km/sec)

FIGURE 19

31.

LOVE WAVE DISPERSION

+ Result of LAH N-S
  comp March 23, 1966

o Calculated from NDI N-S
  Sept. 28, 1966 and ANP N-S
  comp Feb. 5, 1966 by using
  path-weighed regionalization

FIGURE 20

GROUP VELOCITY (km/sec)

PERIOD (sec)
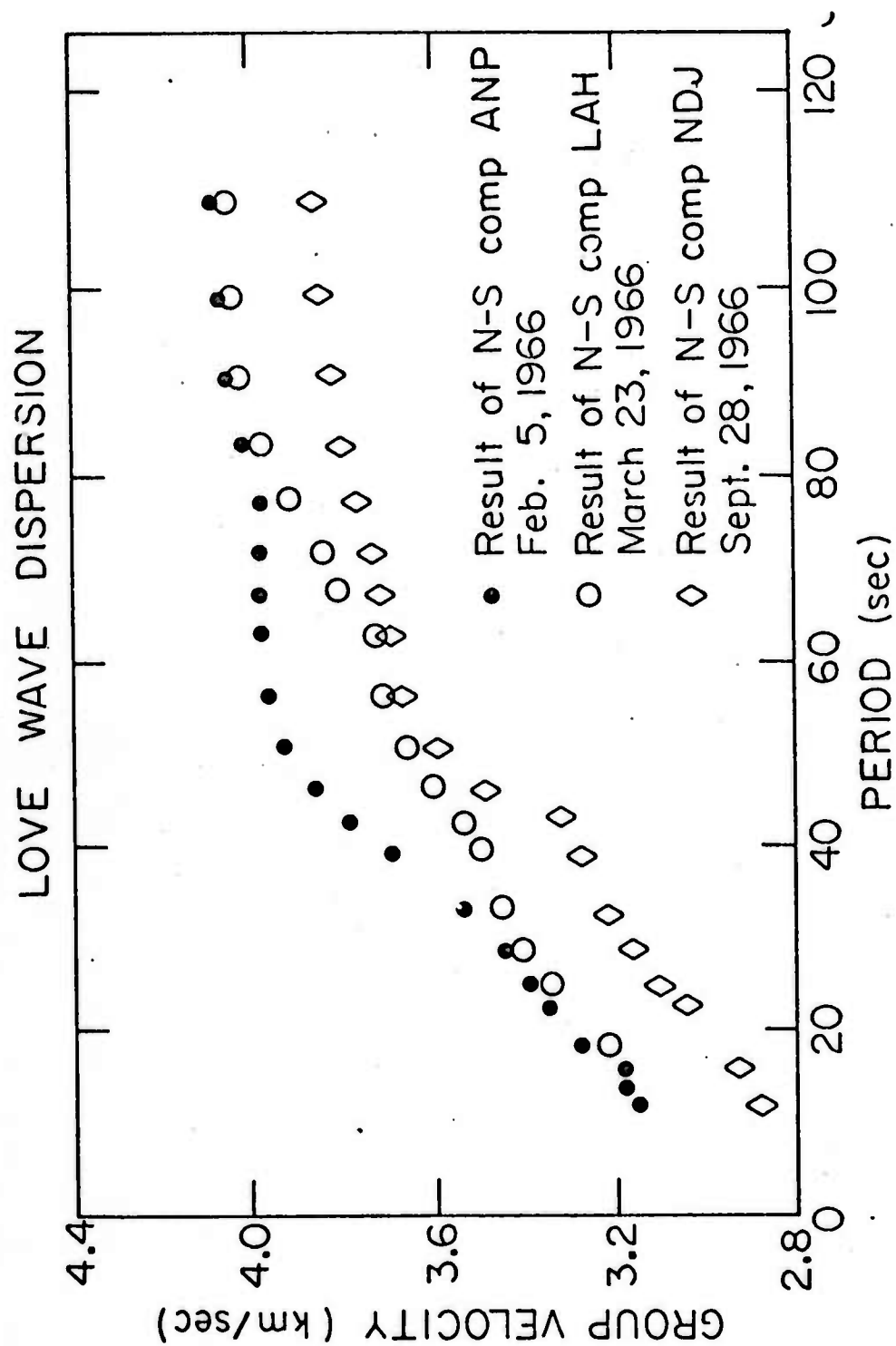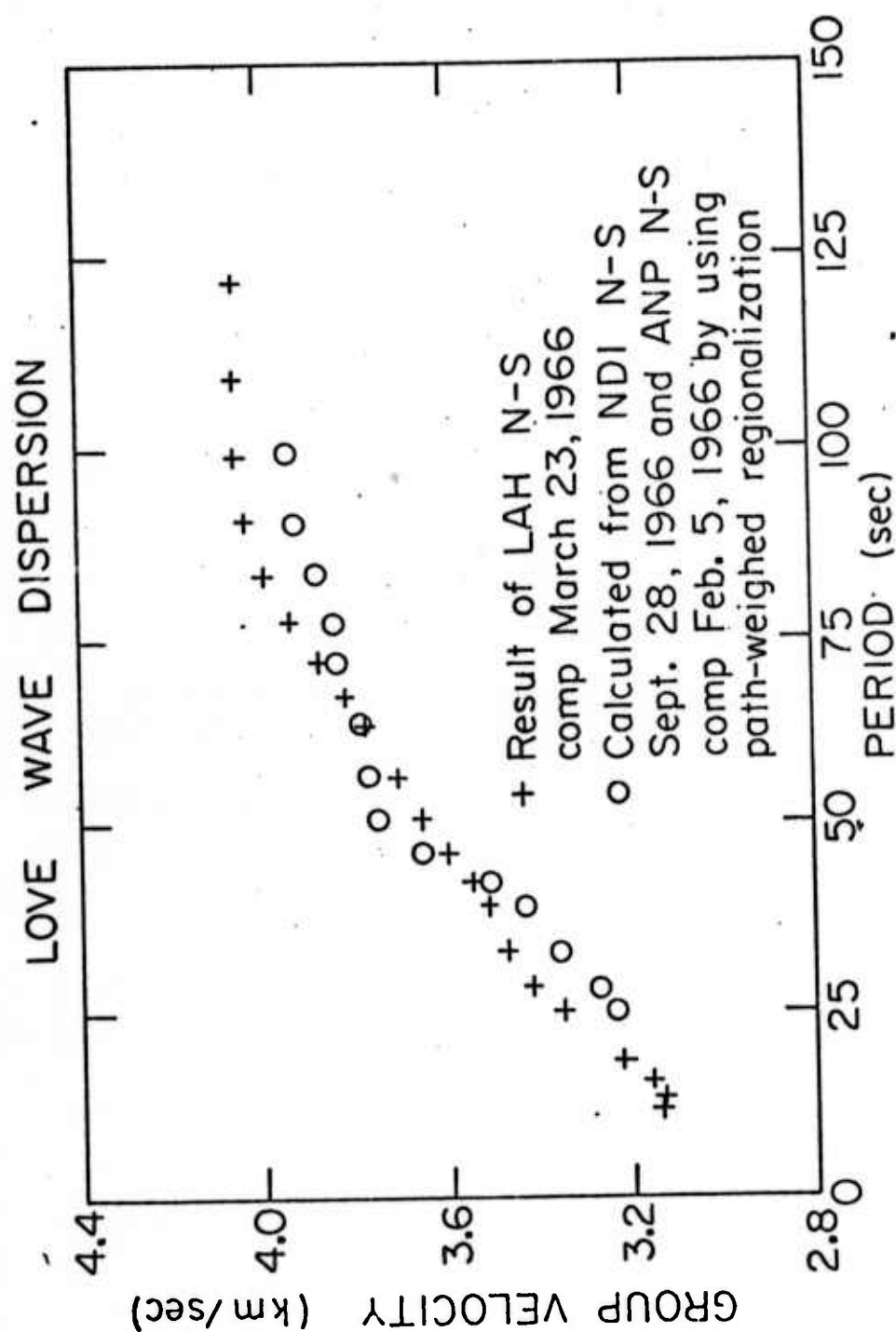
by which the idea of regionalization can be tested. In Figures 18 and 19 there are three sets of dispersion data presented: the bottom set is for the path A, the top set for path B, and the middle set for path C. The data points for path C fall between those for paths A and B as expected, although the present quality of the dispersion data does not allow a further test on the nature of the weighting function. If a linear weight is assigned, as it has been used in the works cited earlier, we have computed a mixed-path dispersion curve (circles in Figure 20) which compares reasonably well with the observed mixed-path dispersion data. One thus can at least conclude that within the experimental errors, the linear path-length weighted mean is a reasonable assumption when the idea of regionalization is applied. In our future surface wave work of the northern China, the mixed-path situation cannot be avoided for the absence of appropriate source-station combination. The method of regionalization will be applied without further justifications.

VII FURTHER WORK IN PROGRESS

The present project has the objective of a systematic surface wave study of the crustal and upper mantle structure of the entire China. What have been reported in the preceeding pages are some of the preliminary results that have been derived from the first six months study under the present contract. And the results reported concern the southern half of the Chinese Mainland. Work is presently being progressed in seeking the crustal and upper mantle information of the northern part of China. Since the approach is quite frutiful and results are very encouraging, it is our intent to extend the study further north to include the Siberia landmass.

VII REFERENCES

Dziewonski, A.,S. Bloch, and M. Landisman; (1969) A Technique for the Analysis of Transient Seismic Signals, Bull. Seism. Soc. Am., V. 59, pp. 427-444.

U.S. Geological Survey (1967; Atlas of Asia and Eastern Europe To Support Detection of Underground Nuclear Testing, 5 Volume.

Cooley, J. W., and J. W. Tukey (1965, An Algorithm for the Machine Calculation of Complex Fouvier Series, Mathematics of Computation, V. 19, pp. 297-301.

Dziewonski, A. M., A. L. Hales (1972). Numerical Analysis of Dispersed Seismic Waves, Methods in Computational Physics, V. 11. Academic Press, 306 p.

Hermann, R.B. (1973) Some Aspects of Band-Pass Filtering of Surface Waves., Bull. Seism. Soc. Am., V. 63. pp 663-671

Papoulis, A. (1962). The Fourier Integral and Its Applications, McGraw-Hill, New York.

Landisman, M. A. Dziewonski, and Y. Sato (1969). Recent Improvements in the Analysis of Surface Wave Observations. Geophys. J. Astr. Soc. V. 17, pp 369-403

Anderson, D.L., A. Ben-Menahem, and C. B. Archambeau, (1965) Attenuation of Seismic Energy in the Upper Mantle, J. Geophys. Res., 70 p. 1441.

Wang, C. Y. (1970) Density and Constitution of the Mantle, J. Geophys. Res. V. 75, p. 3264.

Kanamori, H., (1970) Velocity and Q of Mantle Waves, Phys. Earth Planet. Interiors, 2, 259.

Solomon, S.C. (1972) Seismic-Wave Attenuation and Partial Melting in the Upper Mantle of North America, J. Geophys. Res. V.77, p. 1483.

Tacheuchi, H., and J. Dorman, (1964) Partial Derivatives of Surface Wave Phase Velocity with Respect to Physical Parameter Changes Within the Earth, J. Geophys. Res. V. 69, p. 3429.

Wu, F.T., (1972) Mantle Rayleigh Wave Disoersion and Tectonic Provinces, J. Geophys. Res., V. 77, p. 6445.

Tokosöz, M.N. and D. L. Anderson, (1966) Phase Velocity of Long Period Surface Waves and Structure of the Upper Mantle, J. Geophys. Res. V. 71, p.1649

Hamada, K. (1972) Regionalized Sheer-Velocity Models for the Upper Mantle Inferred from Surface-Wave Dispersion Data, J. Phys. Earth, V. 20, p. 301.

Gutenberg, B. (1955) Channel Waves in theEarth's Crust, V. 20, p. 283.

Molnar, P., T.J. Fitch, and F. T. Wu (1972) Fault plane Solutions of Shallow Earthquakes and Contemporary Tectonics in Asia Phys. Earth Planet., 19, p. 101-112.

Chang, C. F. and S. L. Zeng (1973) Tectonic Features of the Mount Jolmo
    Lungma Region in Southern Tibet,China, Scientia Geologica Sinica., V. 1, p.1.

Press F. (1970), Earth Models Consistent with Geophysical Data, Phys. Earth
    Planet Interiors, 3, p. 1.